Musashino Red Cross Hospital; Eiji Maemura, Department of Neurosurgery, Akiru Municipal General Hospital; Takao Kitahara, Department of Emergency and Critical Care Medicine, Kitasato University School of Medicine; Taiji Makisumi, Internal Medicine, Surgery, Makisumi Memorial Hospital; Kohei Yamashita, Department of Neurosurgery, Sagamihara Central Hospital; Kazunao Onouchi, Department of Neurosurgery, Shimizu Municipal Hospital; Tohichi Nakane, Department of Neurosurgery, Handa Municipal Hospital; Tsunehiko Miyamoto, Department of Neurosurgery, Seirei Mikatabara General Hospital; Takashi Funakoshi, Department of Neurosurgery, Daiyukai General Hospital; Junji Nagata, Department of Neurosurgery, Hamaoka Municipal Hospital; Taro Nakamura, Department of Neurosurgery, TOYOTA Motor Co. TOYOTA Memorial Hospital; Takafumi Saito, Department of Neurosurgery, Nagano Red Cross Hospital; Hidenori Miyake, Department of Neurosurgery, Hamamatsu Rosai Hospital; Yasuhiko Tokuriki, Department of Neurosurgery, Fukui Red Cross Hospital; Kazuyuki Goshima, Department of Internal Medicine, Inazawa City Hospital; Yukio Watanabe, Department of Internal Medicine, Ogaki Municipal Hospital; Takashi Kameyama, Department of Neurology, Gifu Prefectural Tajimi Hospital; Satoshi Okuda, Department of Neurology, Nagoya National Hospital; Takashi Okabe, Department of Neurology, Shizuoka Red Cross Hospital; Toshimasa Sakakibara, Department of Neurology, Labour Welfare Corporation Chubu Rosai Hospital (Industrial Injury Hospital); Chiyuki Mabuchi, Department of Neurology, Nagoya Ekisaikai Hospital; Naoki Sakai, Department of Neurology, Yaizu City Hospital; Yutaka Saitoh, Department of Neurology, Sannomachi Hospital; Koji Kajiyama, Department of Neurology, Kansai Rosai Hospital; Yasumasa Yamamoto, Department of Neurology, Kyoto Second Red Cross Hospital; Kazuo Minematsu, Cerebrovascular Division, Department of Medicine, National Cardiovascular Center; Hiroaki Naritomi, Cerebrovascular Division, Department of Medicine, National Cardiovascular Center; Takeshi Miyashita, Cerebrovascular Department of Internal Medicine, Yodogawa Christian Hospital; Makoto Ogawa, Department of Neurology, Izumisano Municipal Hospital; Shuji Hashimoto, Department of Neurology, Tenri Hospital; Kenichi Oku, Department of Internal Medicine, Division of Cerebro-vascular Disease, Hanwa Memorial Hospital; Jiro Oita, Department of Neurology, Hikone Municipal Hospital; Masayasu Tabuchi, Neurology Service, Hyogo Brain and Heart Center at Himeji; Nobuo Handa, Stroke Unit, Internal Medicine, Hoshigaoka Kouseinenkin Hospital; Shogo Tominaga, Department of Neurosurgery, Yoshida Hospital; Tatsuhito Yamagami, Center for Stroke, Neurosurgical and Neurological diseases, Kyoto Kizugawa Hospital; Tetsuya Tsukahara, Department of Neurosurgery, Kyoto National Hospital; Taira Nishioka, Internal Department, Nishioka Hospital; Takehisa Omura, Department of Neurosurgery, Nishinomiya Kyoritsu Neurosurgical Hospital; Shunichi Yoneda, Department of Neurosurgery, Nipponbashi Hospital; Toshihiro Fukusako, Department of Neurology, Ube Industries LTD. Central Hospital; Chiho Fujii, Department of Acute Medicine, Kawasaki Medical School; Yoshihide Kanehisa, Neurology, Kure Kyosai Hospital; Atsuo Yamada, Department of Neurology, Kure National Hospital; Kiyohiro Sasaki, Department of Neurology, Hamada National Hospital; Etsuko Awaki, Department of Neurology, Saiseikai Sakaiminato General Hospital; Satoshi Yamao, Department of Neurology, Kurasiki Central Hospital; Takeo Yoshimura, Department of Neurology, Neurological Center, Shimonoseki Kosei Hospital; Masahiro Yamasaki, Department of Neurology, Chikamori Hospital; Ikuo Hirata, Department of Internal Medicine, Yamaguchi Prefectural Central Hospital; Kunihiko Osaka, Department of Neurosurgery, Osaka Neurosurgery Hospital; Shunichiro Fujimoto, Department of Neurosurgery, Kagawa Rosai Hospital; Masanori Morimoto, Department of Neurosurgery, Kochi Prefectural Hata Kenmin Hospital; Junichi Imamura, Department of Neurosurgery, Shimonoseki National Hospital; Junji Yoshioka, Department of Neurological Surgery, Okayama Kyokuto Hospital; Norio Sunami, Department of Neurological Surgery, Matsuyama Shimin Hospital; Hideki Hondo, Department of Neurosurgery, Tokushima Prefectural Central Hospital; Noboru Asano, Department of Neurosurgery, Oe Kyodoh General Hospital of Tokushima Prefectural Welfare Federaion of Agricultural Co-operative Associations; Yasuhiro Yamaguchi, Department of Neurology, Arao City Hospital; Naoki Fujii, Department of Neurology, Iizuka Hospital; Miyuki Mori, Stroke Center & Gammma Knife Center, Nagatomi Hospital; Kenji Nakayama, Department of Neurosurgery, Omura City General Hospital; Masaki Tsujimura, Department of Neurosurgery, Kitakyusyu City Yahata Hospital; Tsutomu Masumitsu, Department of Neurosurgery, Taragi Municipal Hospital; Yoichiro Hashimoto, Department of Neurology, Kauamoto City Hospital; Kuniyasu Wada, Department of Neurology, Labour Welfare Corporation Kumamoto Rosai Hospital; Junichi Ikeda, Department of Neurology, Kumamoto Neurosurgical Hospital; Tatsuo Yuge, Department of Neurosurgery Takagi Hospital; Michio Nishikawa, Department of Neurosurgery, Kokura Memorial Hospital; Masayasu Kamouchi, Department of Cerebrovascular Disease, National Kyushu Medical Center; Toshiro Yonehara, Stroke Center, Saiseikai Kumamoto Hospital; Hiroyoshi Imai, Department of Neurology, Federation of National Public Service Personnel Mutual Aid Associations Shinbeppu Hospital; Hitonori Takaba, Division of Cerebrovascular Disorders, St. Mary's Hospital; Kohei Kamimura, Department of Neurology, Tarumizu City Central Hospital; Yoshitomo Ishii, Division of Internal Medicine, Nishiarita Kyoritsu Hospital; Masayuki Atsuchi, Jifukai Medical Corporation, Atsuchi N.S. Hospital.

References

1. Sarti C, Rastenyte DR, Cepaitis Z, et al. International trends in mortality from stroke, 1968 to 1994. Stroke 2000;31:1588-1601.
2. Morikawa Y, Nakagawa H, Naruse Y, et al. Trends in stroke incidence and acute case fatality in a Japanese rural area. The Oyabe study. Stroke 2000;31:1583-1587.
3. Kodama K. Stroke trends in Japan. Ann Epidemiol 1993; 3:524-528.
4. Ministry of Health, Labour and Welfare. Social and economic changes surrounding individuals. Annual Report on Health, Labour and Welfare 2000-2001. Health, Labour and Welfare Administration for Providing Life-Long Support to Self-Sufficiency of the People. Tokyo, Japan, Gyosei Corporation, 2002, 136-150.
5. National Institute of Neurological Disorders and Stroke Ad Hoc Committee. Classification of cerebrovascular diseases III. Stroke 1990;21:637-675.
6. van Swieten JC, Koudstaal PJ, Visser MC, et al. Interobserver agreement for the assessment of handicap in stroke patients. Stroke 1988;19:604-607.
7. Rothrock JF, Lyden PD, Brody ML, et al. An analysis of ischemic stroke in an urban southern California population. The University of California, San Diego, Stroke data bank. Arch Intern Med 1993;153:619-624.
8. Kay R, Woo J, Kreel L, et al. Stroke subtypes among Chinese living in Hong Kong: The Shatin stroke registry. Neurology 1992;42:985-987.
9. Misbach J, Ali W. Stroke in Indonesia: A first large prospective hospital-based study of acute stroke in 28 hospitals in Indonesia. J Clin Neurosci 2001;8:245-249.
10. Yip PK, Jeng JS, Lee TK, et al. Subtypes of ischemic stroke. A hospital-based stroke registry in Taiwan (SCAN-IV). Stroke 1997;28:2507-2512.
11. Bogousslavasky J, Melle GV, Rgli F. The Lausanne stroke registry: Analysis of 1,000 consecutive patients with first stroke. Stroke 1988;19:1083-1092.
12. Yatsu FM, Becker C, McLeroy KR, et al. Community hospital based stroke programs: North Carolina, Oregon, and New York I: Goals, objectives and data collection procedures. Stroke 1986;17:276-284.
13. Brutto OHD, Mosquera A, Sanchez X, et al. Stroke subtype Hispanics living from Guayaquil, Ecuador. Results from the Luis Vernaza hospital stroke registry. Stroke 1993;24:1833-1836.
14. Lee BI, Nam HS, Heo JH, et al and the Yonei stroke team. Yonsei stroke registry. Cerebrovasc Dis 2001;12:145-151.
15. Foulkes MA, Wolf PA, Price TR, et al. The stroke data bank: Design, methods, and baseline characteristics. Stroke 1988;19:547-554.
16. Tanizaki Y, Kiyohara Y, Kato I, et al. Incidence and risk factors for subtypes of cerebral infarction in a general population. The Hisayama study. Stroke 2000;31:2616-2622.
17. Petty GW, Brown Jr RD, Whisnant JP, et al. Ischemic stroke subtype. A population-based study of incidence and risk factors. Stroke 1999;30:2513-2516.
18. Kolominisky-Rabas PL, Weber M, Gefeller O, et al. Epidemiology of ischemic stroke subtypes according to TOAST criteria. Incidence, recurrence, and long-term survival in ischemic stroke subtype: A population-based study. Stroke 2001;31:2735-2740.
19. Friday G, Lai SM, Alter M, et al. Stroke in the Lehigh Valley: Racial/ethnic differences. Neurology 1989;39: 1165-1168.
20. Wester P, Radberg J, Lundgren B, et al for the Seek-Medical-Attention-in-Time Study Group. Factor associated with delayed admission to hospital and in hospital delays in acute stroke and TIA. A prospective, multicenter study. Stroke 1999;30:40-48.
21. Indredavik B, Bakke F, Slordahl SA, et al. Stroke unit treatment improve long-term quality of life. A randomized controlled trial. Stroke 1998;29:895-899.
22. Ronning OM, Guldvog B. Stroke unit versus general ward, I: Twelve-and eighteen-month survival. A randomized controlled trial. Stroke 1998;29:58-62.
23. Ronning OM, Guldvog B. Stroke unit versus general ward, II: Neurological deficits and activities of daily living. A Quasi-randomized controlled trial. Stroke 1998; 29:586-590.
24. Adams HP, Davis PH, Leira EC, et al. Baseline NIH stroke scale score strongly predicts outcome after stroke. A report of the trial of Org 10172 in acute stroke treatment (TOAST). Neurology 1999;53:126-131.
25. Minematsu K, Yamaguchi K, Omae T. Spectacular shrinking deficit: Rapid recovery from a major hemispheric syndrome by migration of an embolus. Neurology 1992;42:157-162.
26. National Institute of Neurological Disorders and Stroke rt-PA stroke Study Group. Tissue plasminogen activator for acute ischemic stroke. N Engl J Med 1995;333:1581-1587.
27. Hacke W, Kaste M, Fieschi C, et al for the ECASS Study Group. Intravenous thrombolysis with recombinant tissue plasminogen activator for acute hemispheric stroke: The European Cooperative Acute Stroke Study (ECASS). JAMA 1995;274:1017-1025.
28. Barber PA, Zhang J, Demchuk AM, et al. Why are stroke patients excluded from TPA therapy? An analysis of patients' eligibility. Neurology 2001;56:1015-1020.
29. Chiu D, Krieger D, Villar-Cordova C, et al. Intravenous tissue plasminogen activator for acute ischemic stroke: Feasibility, safety, and efficacy in the first year of clinical practice. Stroke 1998;29:18-22.
30. Bornstein NM, Aronovich BD, Karepov VG, et al. The Tel Aviv stroke registry 3600 consecutive patients. Stroke 1996;27:1770-1773.
31. Frey JL, Jahnke HK, Bulfinch EW. Differences in stroke between White, Hispanic and native American patients. The Barrow Neurological Institute stroke database. Stroke 1998;29:29-33.
32. Feigin VL, Wiebers DO, Nikitin YP, et al. Risk factors for ischemic stroke in a Russian community. A population-based case-control study. Stroke 1999;29:34-39.
33. Smadja D, Cabre P, May F, et al and the ERMANCIA study group. ERMANCIA: Epidemiology of stroke in Martinique, French West Indies. Stroke 2001;32:2741-2747.
34. Sacco RL, Benjamin CEJ, Broderick JP, et al. Risk factors. Stroke 1997;28:1507-1517.
35. Summary of the National Cholesterol Education Program (NCEP) Adult Treatment Panel II report. JAMA 1993;269:3015-3023.
36. Bonita R, Boad JB, Beaglehole R. Changes in stroke incidence and case-fatality in Auckland, New Zealand, 1981-91. Lancet 1993;342:1470-1473.
37. Stegmayr B, Asplund K, Wester PO. Trends in incidence, case-fatality rate, and severity of stroke in Northern Sweden, 1985-1991. Stroke 1994;25:1738-1745.
38. Hong Y, Bots ML, Pan X, et al. Stroke incidence and mortality in rural and urban Shanghai from 1984 through 1991. Findings from a community-based registry. Stroke 1994;25:1165-1169.
39. Korv J, Roose M, Kaasik AE. Changed incidence and case-fatality rates of first-ever stroke between 1970 and 1993 in Tartu, Estonia. Stroke 1996;27:199-203.

Characterisation of [^{123}I]iomazenil distribution in a rat model of focal cerebral ischaemia in relation to histopathological findings

Tomohito Kaji[1], Yuji Kuge[2], Chiaki Yokota[3], Masafumi Tagaya[5], Hiroyasu Inoue[4], Tohru Shiga[1], Kazuo Minematsu[6], Nagara Tamaki[1]

[1] Department of Nuclear Medicine, Hokkaido University Graduate School of Medicine, Kita-ku, Sapporo, Japan
[2] Department of Tracer Kinetics, Hokkaido University Graduate School of Medicine, Kita-ku, Sapporo, Japan
[3] Department of Pathogenesis, Research Institute, National Cardiovascular Center, Suita, Osaka, Japan
[4] Department of Pharmacology, Research Institute, National Cardiovascular Center, Suita, Osaka, Japan
[5] Department of Internal Medicine, National Osaka Hospital, Chuo-ku, Osaka, Japan
[6] Cerebrovascular Division, Department of Medicine, National Cardiovascular Center, Suita, Osaka, Japan

Received: 14 May 2003 / Accepted: 27 July 2003 / Published online: 8 October 2003

Abstract. Iodine-123 labelled iomazenil ([^{123}I]IMZ) has been reported to be a useful marker of neuronal viability. The brain distribution of [^{123}I]IMZ, however, has not been correlated with the pathophysiological response in detail after an ischaemic insult. To characterise [^{123}I]IMZ as a marker of neuronal viability, we compared its brain distribution with cyclooxygenase-2 (COX-2) expression, DNA fragmentation and cellular integrity. [^{123}I]IMZ and [^{125}I]IMP were injected into rats with focal cerebral ischaemia for the purpose of dual-tracer autoradiography. COX-2 and microtubule-associated protein-2 (MAP-2, a marker of cellular integrity) were immunostained. In situ DNA polymerase-I-dependent dUTP incorporation into damaged DNA was used as an indicator of DNA fragmentation. Lesion to normal ratios (LNRs) for [^{123}I]IMP and [^{125}I]IMZ were calculated. [^{123}I]IMZ accumulation was preserved in several regions with impaired [^{123}I]IMP accumulation. COX-2 expression was occasionally observed, whereas neither DNA fragmentation nor MAP-2 denaturation was detected in these regions. DNA fragmentation and impaired MAP-2 immunostaining were observed only in the regions with reduced LNRs for both tracers. The LNR for [^{123}I]IMZ was significantly lower in regions with impaired MAP-2 immunostaining (0.120±0.152, $P<0.0001$), in regions positive for dUTP incorporation (0.488±0.166, $P<0.0001$) and in regions positive for COX-2 expression (0.626±0.186, $P<0.001$) than in histologically normal regions (0.784±0.213). Thus, neuronal DNA is still intact and cellular integrity is maintained in the ischaemic regions with preserved [^{123}I]IMZ accumulation. The impairment of [^{123}I]IMZ accumulation precedes DNA fragmentation and denaturation of cellular integrity. These results provide the molecular basis of [^{123}I]IMZ distribution.

Keywords: [^{123}I]iomazenil – Cerebral ischaemia – Neuronal viability – Cyclooxygenase-2 – DNA fragmentation

Eur J Nucl Med Mol Imaging (2004) 31:64–70
DOI 10.1007/s00259-003-1319-6

Nagara Tamaki (✉)
Department of Nuclear Medicine,
Hokkaido University Graduate School of Medicine,
Kita 15 Nishi 7, 060-8638 Kita-ku, Sapporo, Japan
e-mail: natamaki@med.hokudai.ac.jp
Tel.: +81-11-7065150, Fax: +81-11-7067155

Introduction

An ischaemic stroke is one of the most common neuronal disorders, and the number of patients suffering from the disease is increasing. For the clinical evaluation of ischaemic stroke, it is very important to precisely detect the ischaemic penumbra, which is an ischaemically affected but still viable tissue, because the penumbral tissue can be salvaged by pharmacological and/or surgical interventions [1, 2, 3, 4].

Iodine-123 iomazenil ([^{123}I]IMZ) is a probe for central-type benzodiazepine receptor (BZR) for single-photon emission tomography (SPET). Since GABA receptors are abundant in the cortex and sensitive to ischaemic damage, specific radioligands to their subunits, the cerebral BZRs existing in GABA-A receptors, can be used as a marker of neuronal viability [5]. Thus, BZR imaging with [^{123}I]IMZ should be useful for detecting viable neurons, which may help detect the penumbra after an isch-

aemic insult. In this regard, several experimental and clinical investigators have compared the [^{123}I]IMZ distribution with the cerebral blood flow, oxygen metabolism and/or glucose metabolism, and shown the potential of [^{123}I]IMZ for evaluation of neuronal viability after an ischaemic stroke [3, 6, 7, 8, 9, 10, 11, 12]. A few authors [6, 10, 11] have also correlated [^{123}I]IMZ distribution with histological findings obtained using the haematoxylin-eosin stain.

To the best of our knowledge, however, the brain distribution of [^{123}I]IMZ has not been correlated with the molecular response after an ischaemic insult in detail. The pathophysiological significance of findings that are actually imaged by [^{123}I]IMZ also remains to be elucidated. Accordingly, we compared the brain distribution of [^{123}I]IMZ with (1) cerebral blood flow, (2) the expression of cyclooxygenase-2 (COX-2), (3) fragmentation of DNA and (4) cellular integrity, in order to characterise [^{123}I]IMZ as a marker of neuronal viability. COX-2, a prostanoid synthesising enzyme, is expressed early after an ischaemic insult and contributes to the progression of ischaemic damage [13, 14, 15, 16, 17]. Thus, we examined COX-2 expression to evaluate the neuronal response early after an ischaemic insult. In situ DNA polymerase-I-dependent dUTP incorporation into damaged DNA was used as an indicator of DNA fragmentation. Techniques for visual detection and localisation of DNA injury/repair in situ include: TdT-dependent dUTP labelling of free 3'-OH ends of double-stranded DNA (TUNEL); Klenow fragment of DNA polymerase-I-dependent labelling of staggered 3'-OH ends and gaps; and DNA polymerase-I incorporation in nicks, gaps and staggered 3'-OH ends [18]. Of these, only DNA polymerase-I has 5'–>3' exonucleolytic activity, which allows nick translation and visualisation of randomly occurring single-strand scission of double-stranded DNA. MAP-2, a cellular structural protein existing on the surface of neurodendrites, is also immunostained as a marker of cellular integrity.

Materials and methods

Animal preparation. The experimental protocol was fully approved by the Laboratory Animal Care and Use Committee of Hokkaido University. Male Sprague-Dawley rats weighing 300–350 g were used. The rats had free access to water and laboratory chow. The animals were initially anaesthetised with 400 mg/kg body weight IP chloral hydrate. The body temperatures were monitored with rectal probes and maintained at 37°C with heating pads during the operation. The rats were subjected to permanent unilateral major artery occlusion. The right middle cerebral artery (MCA) of each rat was occluded intraluminally according to a method described in detail previously [19, 20, 21]. The rats were allowed to recover from anaesthesia and any induced neurological deficits were confirmed. The animals not showing any neurological deficits were excluded from this experiment.

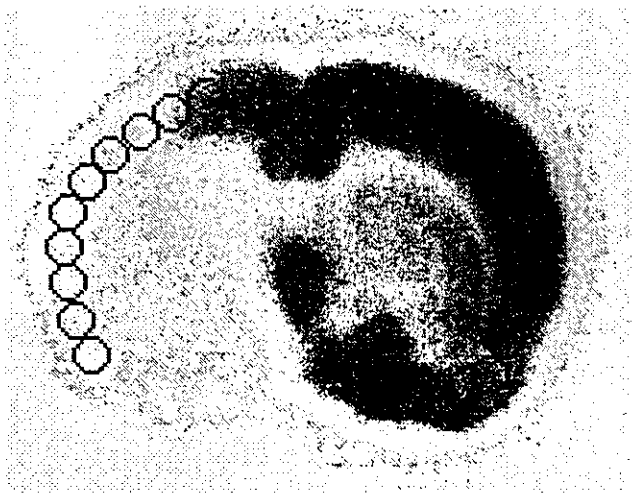

Fig. 1. An example of regions of interest (ROIs) on a coronal image. Twelve circular ROIs (2 mm in diameter) were determined on each hemisphere of the cortex symmetrically

Autoradiographic studies. The brain distributions of [^{123}I]IMZ and [^{125}I]IMP were determined using a dual-tracer autoradiographic technique. [^{123}I]IMZ (111 MBq/kg body weight) was first injected via the femoral vein 60 min before decapitation, to determine specific [^{123}I]IMZ distribution according to the methods reported by Toyama et al. [10, 11]. Then, 55 min later, [^{125}I]IMP (2.22 MBq/kg body weight) was injected via the contralateral femoral vein, to assess blood flow distribution [10, 11]. The rats were decapitated under chloral hydrate anaesthesia 5 min after the injection of [^{125}I]IMP, which was 2, 3, 4, 6, 8, 12 and 24 h after the ischaemic insult (n = four to six in each group). Their brains were removed quickly and carefully, and immersed in ice-cold saline. The brains were then sectioned at 6 mm caudal from the frontal pole using a brain matrix (RBM-4000C, ASI Instruments, Warren, MI) to obtain coronal sections. The brain samples were embedded in a medium (Tissue-Tek, Sakura Finetechnical Co., Ltd., Tokyo, Japan), frozen in isopentane-dry ice, and cut into 20-μm sections with a cryostat (Bright Instrument Co., Ltd., Cambridgeshire, England). The first autoradiographic exposure was performed for 3 h to detect the distribution of [^{123}I]IMZ. The second exposure was initiated 7 days later and carried out for 7 days to visualise the distribution of [^{125}I]IMP.

Histological studies. Immunoreactivity to COX-2 and microtubule-associated protein-2 (MAP-2) were detected in frozen sections (10 μm thick) adjacent to those used for the autoradiographic studies, using a standard immunostaining procedure [23]. Briefly, after fixation in a cold 1:1 acetone-to-methanol mixture, the sections were incubated with a polyclonal anti-COX-2 antibody (Cayman Chemical; dilution 1:2,000) or a purified mouse monoclonal anti-MAP-2 antibody (BD Pharmingen, San Diego; dilution 1:400). The bound antibody was visualised by staining with avidin/biotin conjugate immunoperoxidase (Vector Laboratories, Inc., CA, USA) and 3,3'-diaminobenzidine tetrahydrochloride (DAB; Vectastain Elite Kit, Vector Laboratories, CA).

DNA fragmentation was also detected on the adjacent sections by incorporation of digoxigenin-dUTP using DNA polymerase-I according to the method previously described [18, 23]. To confirm the nuclear localisation of the label, some sections were counterstained with haematoxylin.

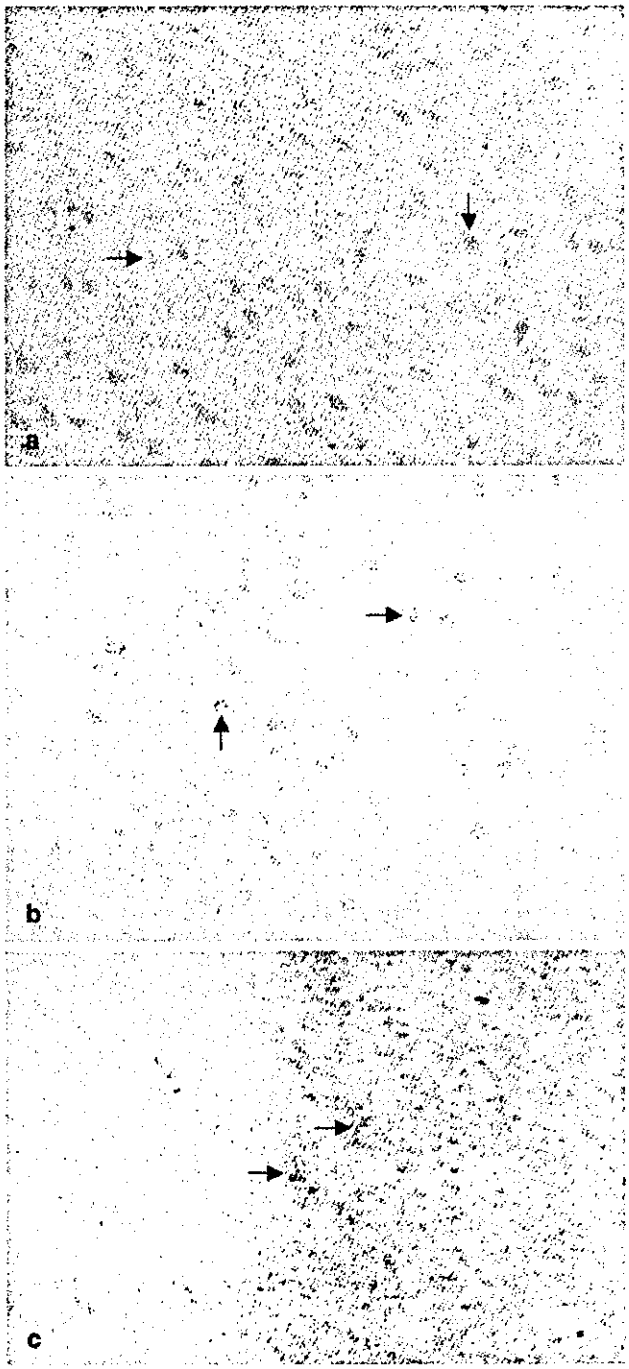

Data analysis. The autoradiograms were analysed using a computerised imaging analysis system (Bio-imaging Analyser BAS-5000, Fuji Photo Film, Tokyo, Japan). To quantitatively evaluate the distributions of [^{123}I]IMZ and [^{125}I]IMP, 12 circular regions of interest (ROIs, 2 mm in diameter) were determined on each hemisphere of the cerebral cortex in the autoradiograms symmetrically from the longitudinal fissure to the temporal lobe (Fig. 1). Lesion to normal ratios (LNRs) were defined as the ratios of values for an ROI in the lesioned hemisphere to those for the contralateral homologous ROI.

Based on the LNRs for [^{123}I]IMZ and [^{125}I]IMP, ROIs determined on the lesioned hemisphere were classified into three groups as shown in Table 1: group 1, LNRs for both [^{125}I]IMP and [^{123}I]IMZ were equal to or larger than 0.8; group 2, the LNRs for [^{125}I]IMP were less than 0.8 and those for [^{123}I]IMZ were equal to or larger than 0.8; group 3, LNRs for both [^{125}I]IMP and [^{123}I]IMZ were less than 0.8. A threshold LNR of 0.8 was chosen, considering the lesion detectability by the autoradiographic methods [11].

The ROIs determined on the lesioned hemisphere were also classified into four groups based on histological findings as follows (Fig. 2): group A, impaired MAP-2 immunostaining; group B, preserved MAP-2 immunostaining and positive for dUTP incorporation; group C, preserved MAP-2 immunostaining, negative for dUTP incorporation and positive for COX-2; group D, no histological evidence of an ischaemic injury.

All values are expressed as means or means ± standard deviation. A Z test was used to assess the significance of difference in the percentage of ROIs with impaired [^{125}I]IMP or [^{123}I]IMZ accumulation. One-way ANOVA and post-hoc tests (Fisher's method) were used to assess the significance of difference in the LNRs among the four groups classified on the basis of histological findings. A two-tail value of $P<0.05$ was considered to indicate statistical significance.

Results

Figure 3 shows representative autoradiograms for [^{125}I]IMP and [^{123}I]IMZ. The accumulation of [^{125}I]IMP decreased in a wide region in the MCA territory 2 h after occlusion, which extended with time. The region with

Fig. 2a–c. Representative images of **a** COX-2 immunostaining (×200), **b** dUTP incorporation (×200) and **c** MAP-2 immunostaining (×200). **a** Expression of COX-2 protein was occasionally observed (*arrows*). **b** The ring-like appearance (*arrows*) of dUTP incorporation shows the neuron on the way to apoptotic cell death. **c** Positive MAP-2 immunostaining (*arrows*) shows cellular integrity

Table 1. Histological findings in the three ROI groups classified on the basis of LNRs

Group	LNR_{IMP}	LNR_{IMZ}	Number (%) of ROIs		
			COX-2 (+)	dUTP (+)	MAP-2 (–)
Group 1 (n=14)	≥0.8	≥0.8	0 (0%)	0 (0%)	0 (0%)
Group 2 (n=24)	<0.8	≥0.8	4 (16.7%)	0 (0%)	0 (0%)
Group 3 (n=238)	<0.8	<0.8	79 (33.2%)	59 (24.8%)	176 (73.9%)

LNR_{IMP}, LNR for [^{125}I]IMP; LNR_{IMZ}, LNR for [^{123}I]IMZ; COX-2 (+), positive immunostaining for COX-2; dUTP (+), positive dUTP incorporation; MAP-2 (–), negative immunostaining for MAP-2

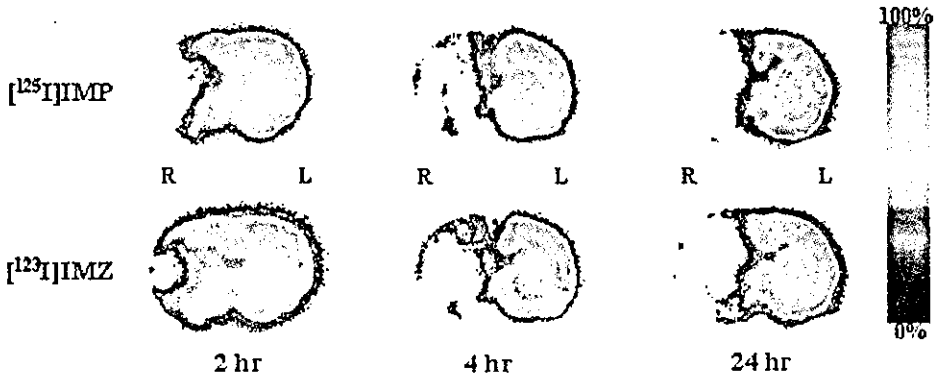

Fig. 3. Representative autoradiograms for [125I]IMP and [123I]IMZ

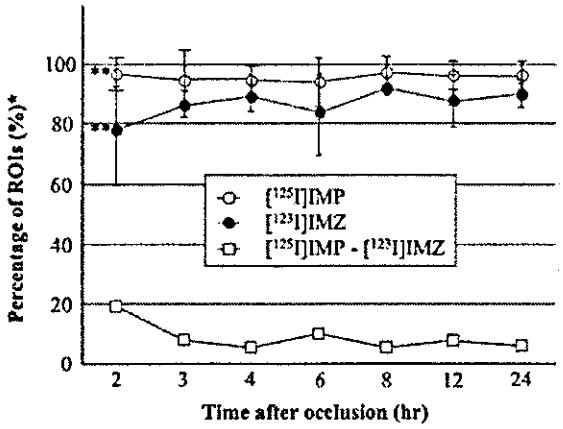

Fig. 4. Time course of the percentage of ROIs with impaired [125I]IMP or [123I]IMZ accumulation. *(Number of ROIs with LNRs less than 0.8)/(Number of total ROIs at each time point) ×100. ROIs with impaired [125I]IMP and [123I]IMZ accumulation were defined as those with LNRs less than 0.8. Significant uncoupling of accumulation between the two tracers was observed 2 h after occlusion (**P<0.01)

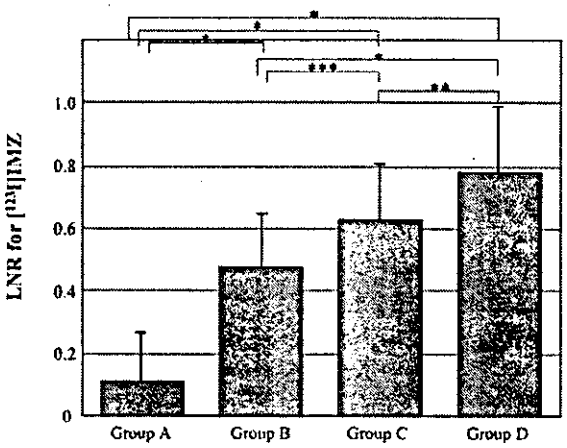

Fig. 5. The LNRs for [123I]IMZ in the four ROI groups classified on the basis of histological findings. Group A, impaired MAP-2 immunostaining; group B, preserved MAP-2 immunostaining and positive dUTP incorporation; group C, preserved MAP-2 immunostaining, negative dUTP incorporation and positive COX-2 immunostaining; group D, no histological evidence of ischaemic injury. Significant differences in LNRs between two groups: *P<0.0001, **P<0.001, ***P<0.01

decreased [123I]IMZ accumulation was smaller than that with decreased [125I]IMP accumulation (P<0.01). Uncoupling between [125I]IMP and [123I]IMZ accumulation was observed in regions surrounding the ischaemic core 2 h after occlusion, but such uncoupling reduced with time. The percentage of ROIs with impaired [123I]IMZ accumulation was significantly lower than that with decreased [125I]IMP accumulation at 2 h after occlusion (P<0.01), but not at other time points (Fig. 4).

Positivity for COX-2 was observed in 16.7% of the ROIs in the ischaemic lesions with preserved [123I]IMZ distribution (group 2) and 33.2% of the ROIs in the ischaemic lesions with decreased [123I]IMZ distribution (group 3), whereas no positivity for COX-2 was seen in non-ischaemic lesions (group 1) (Table 1). Neither positivity for dUTP incorporation nor decreased immunostaining of MAP-2 was observed in the ROIs in the lesions with preserved [123I]IMZ distribution (groups 1 and 2). Positivity for dUTP incorporation and impaired MAP-2 immunostaining were observed in 24.8% and 73.9% of the ROIs, respectively, in the lesions with decreased [123I]IMZ distribution (group 3) (Table 1).

When the ROIs were divided into four groups based on the histological findings (Fig. 5), the LNRs for [123I]IMZ in the lesions with preserved MAP-2 immunostaining (groups B, C and D) were significantly higher than those in the lesions with impaired MAP-2 immunostaining (group A; P<0.0001). The LNRs for [123I]IMZ in the lesions with preserved MAP-2 immunostaining and positive for dUTP incorporation (group B) were significantly lower than those in the lesions with preserved MAP-2 immunostaining and negative for dUTP incorporation (groups C; P<0.01, group D; P<0.0001). The LNRs for [123I]IMZ in the lesions with preserved MAP-2 immunostaining, negative for dUTP incorporation and positive for COX-2 (group C) were significantly lower

than those in the lesions with no histological evidence of an ischaemic injury (group D; $P<0.001$).

Discussion

In order to characterise [^{123}I]IMZ as a marker of neuronal viability, we compared the brain distribution of [^{123}I]IMZ with the expression of COX-2, DNA fragmentation and cellular integrity. Neither DNA fragmentation nor MAP-2 denaturation was detected in the ischaemic regions with preserved [^{123}I]IMZ accumulation. These results clearly demonstrate that neuronal DNA is still intact and cellular integrity is maintained in the ischaemic regions with preserved [^{123}I]IMZ accumulation. COX-2 expression was often observed in these regions. In addition, semiquantitative analysis based on the histological findings showed that [^{123}I]IMZ accumulation was significantly impaired in regions where DNA fragmentations were observed. Thus, [^{123}I]IMZ distribution can be an indicator that predicts the extent of neuronal damage after an ischaemic stroke.

In the present study, we compared the brain distribution of [^{123}I]IMZ with (1) CBF, (2) the expression of COX-2, a prostanoid synthesising enzyme that contributes to the progression of ischaemic damage [13, 14, 15, 16, 17], (3) fragmentation of DNA and (4) cellular integrity. The regions with preserved [^{123}I]IMZ accumulation and decreased [^{125}I]IMP accumulation, namely, uncoupling between CBF and BZR function, were observed 2 h after occlusion in regions surrounding the ischaemic core, which became smaller with time. Such uncoupling has been observed in the acute phase by several authors [9, 24, 25]. The BZR function in these regions can be regarded as intact in spite of hypoperfusion. Clinically, it was reported that the hypoperfused regions with preserved [^{123}I]IMZ accumulation do not develop infarction as determined in a follow-up evaluation with magnetic resonance imaging [3]. The uncoupling between [^{125}I]IMP and [^{123}I]IMZ accumulation may help determine the ischaemic penumbra.

Some authors [6, 10, 11] have compared [^{123}I]IMZ distribution with histological findings obtained using the haematoxylin-eosin stain. They suggested the potential of [^{123}I]IMZ for evaluating the extent of neuronal damage. The brain distribution of [^{123}I]IMZ, however, has not been correlated with the cellular response at the molecular level. The present results on the relationship between [^{123}I]IMZ accumulation and dUTP incorporation clearly demonstrate that neuronal DNA is still intact in the ischaemic regions where [^{123}I]IMZ accumulation is preserved. In addition, our results indicate the potential of [^{123}I]IMZ to significantly detect the region with DNA scission as a reduction in LNRs. It was reported that COX-2 is expressed early after an ischaemic insult and leads ischaemic neurons to apoptotic cell death [17, 26]. In the present study, COX-2 expression was often observed in the ischaemic regions with preserved [^{123}I]IMZ accumulation. COX-2 expression may precede impairment of [^{123}I]IMZ accumulation. On the other hand, the COX-2 protein was also observed in the regions where [^{123}I]IMZ accumulation decreased. The LNRs for [^{123}I]IMZ accumulation in group C (0.626±0.186) were significantly lower than those in group D (0.783±0.213). The role of the COX-2 protein may begin before the impairment of BZR function and it may continue even after this impairment, although further investigations are required to clarify this point. These results indicate that impairment of [^{123}I]IMZ accumulation may begin as early as the COX-2 expression after an acute stroke.

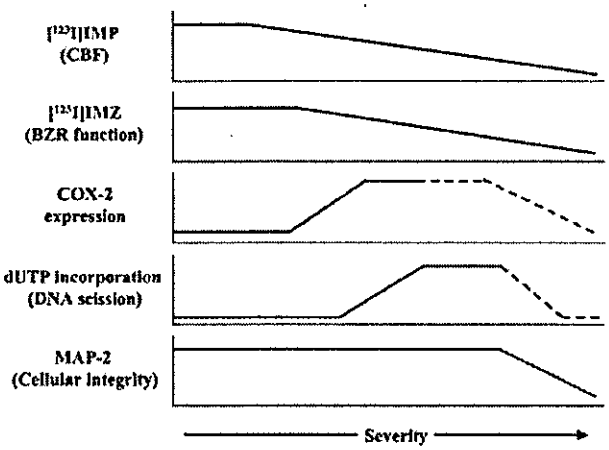

Fig. 6. Schematic representation of possible relationship between tracer accumulation and pathophysiological changes

From our results, a possible relationship between tracer accumulation and pathophysiological changes can be summarised as shown in Fig. 6. Namely, [^{125}I]IMP accumulation decreases concurrently with CBF after an ischaemic insult. COX-2 expression is often observed early after the ischaemic insult. [^{123}I]IMZ accumulation, namely, the BZR function, was impaired at a similar stage to COX-2 expression. DNA scission and impairment of cellular integrity follow the reduction in [^{123}I]IMZ accumulation.

Methodological considerations

In a clinical setting, an interval of several hours is required to sufficiently characterise BZR distribution after the [^{123}I]IMZ injection. In this study, however, rats were sacrificed 60 min after [^{123}I]IMZ administration, according to the method reported by Toyama et al. [10]. Their kinetic study indicated that specific binding of [^{123}I]IMZ can be evaluated 60 min after [^{123}I]IMZ injection in a rat model of cerebral ischaemia. Specific distribution of [^{123}I]IMZ can be achieved in a shorter period of 60 min in rats.

The relationship between tracer distribution and histological findings was evaluated simultaneously using all samples obtained from rats sacrificed at variable time intervals after the ischaemic insult, in order to characterise [^{123}I]IMZ distribution in regions with ischaemic injury of various extent. Regional analysis in rats subjected to the same period of MCA occlusion may provide more precise information on the relationship. The relatively narrow penumbra in rats, however, may restrict such evaluation and require a higher number of rats. Thus, in the present study, the relationship was evaluated simultaneously in rats sacrificed at variable time intervals.

The average LNR for [^{123}I]IMZ in histologically normal regions was not higher than 0.8. Although, in this study, we chose 0.8 as the threshold value of the LNRs for [^{123}I]IMZ, further examinations may be needed to determine a more suitable threshold value of LNR for [^{123}I]IMZ.

In the present study, we used a dual-tracer autoradiographic technique to evaluate the blood flow and [^{123}I]IMZ binding in the same individuals. Consequently, we could not perform quantitative assessment of the blood flow and [^{123}I]IMZ binding, as it is methodologically difficult to quantitatively assess flow and IMZ binding using the dual-tracer autoradiographic technique. Further studies, especially on quantitative measurement of flow and [^{123}I]IMZ binding, are required to confirm the present results and to obtain relevant information on the flow and [^{123}I]IMZ binding in relation to the histopathological findings.

Clinical implications

The routine use of nuclear medicine for the clinical assessment of neuronal viability has been limited exclusively to the determination of CBF, oxygen and/or glucose consumption, and CBF reactivity to acetazolamide. Oxygen and glucose metabolism and CBF reactivity to acetazolamide, however, do not provide direct information on neuronal viability. Rather, these techniques yield information not only on neurons but also on astrocytes and Schwann cells. On the other hand, [^{123}I]IMZ, a central-type BZR ligand, can be a specific marker of neuronal viability. Heiss et al. suggested that imaging of BZR receptors could distinguish between irreversibly damaged and viable penumbra tissues immediately after an acute stroke using carbon-11 flumazenil and positron emission tomography [27, 28]. The present study in the rat model demonstrated that [^{123}I]IMZ can also be a marker for neuronal viability. In addition, [^{123}I]IMZ does not require in-house cyclotrons and positron emission tomography, and can be commercially supplied. The availability of this procedure is expected to favour the clinical application of [^{123}I]IMZ.

Conclusion

The present study demonstrated for the first time that impairment of [^{123}I]IMZ accumulation precedes DNA fragmentation and denaturation of cellular integrity. Our results provide the molecular basis of [^{123}I]IMZ distribution. [^{123}I]IMZ accumulation can be a clue to predicting the severity of ischaemic neuronal injury.

Acknowledgement. The authors are grateful to Professors S. Nishi, K. Miyasaka and T. Ohnishi of the Central Institute of Isotope Science, Hokkaido University, for supporting this work. We also express gratitude to Drs. T. Abumiya and K. Hikosaka for helpful discussions.

This work was supported in part by a Grant-in-Aid for Scientific Research from the Japan Society for the Promotion of Science, and Grants from Japan Heart Foundation Research, the Takeda Medical Research Foundation in Japan and the Mitubishi Pharma Research Foundation in Japan.

References

1. Garcia JH, Lassen NA, Weiller C, Sperling B, Nakagawara J. Ischemic stroke and incomplete infarction. *Stroke* 1996; 27:761–765.
2. Garcia JH, Liu KF, Ye ZR, Gutierrez JA. Incomplete infarct and delayed neuronal death after transient middle cerebral artery occlusion in rats. *Stroke* 1997; 28:2303–2310.
3. Nakagawara J, Sperling B, Lassen NA. Incomplete brain infarction of reperfused cortex may be quantitated with iomazenil. *Stroke* 1997; 28:124–132.
4. Heiss WD, Graf R, Fujita T, Ohta K, Bauer B, Lötten J, Wienhard K. Early detection of irreversibly damaged ischemic tissue by flumazenil positron emission tomography in cats. *Stroke* 1997; 28:2045–2052.
5. Heiss WD, Kracht LW, Thiel A, Grond M, Pawlik G. Penumbral probability thresholds of cortical flumazenil binding and blood flow prediction tissue outcome in patients with cerebral ischaemia. *Brain* 2001; 124:20–29.
6. Odano I, Miyashita K, Minoshima S, Nakajima T, Fujita M, Takahashi N, Ikuta F. A potential use of a ^{123}I-labeled benzodiazepine antagonist as a predictor of neuronal call viability: comparisons with ^{14}C-labeled 2-deoxyglucose autoradiography and histological examination. *Nucl Med Commun* 1996; 16:443–446.
7. Matsuda H, Tsuji S, Kuji I, Shiba K, Hisada K, Mori H. Dual-tracer autoradiography using ^{125}I-iomazenil and ^{99m}Tc-HMPAO in experimental brain ischemia. *Nucl Med Commun* 1995; 16:581–590.
8. Hatazawa J, Shimosegawa E, Satoh T, Kanno I, Uemura K. Central benzodiazepine receptor distribution after subcortical hemorrhage evaluated by means of [^{123}I]IMZ and SPECT. *Stroke* 1995; 26:2267–2271.
9. Dong Y, Fukuyama H, Nabatame H, Yamauchi H, Shibasaki H, Yonekura Y. Assessment of benzodiazepine receptors using iodine-123-labeled iomazenil single-photon emission computed tomography in patients with ischemic cerebrovascular disease. A comparison with PET study. *Stroke* 1997; 28:1776–1782.
10. Toyama H, Matsumura K, Nakashima H, Takeda K, Takeuchi A, Koga S, Yoshida T, Ichise M. Characterization of neuronal

damage by iomazenil binding and cerebral blood flow in an ischemic rat model. *Ann Nucl Med* 1998; 12:267–273.
11. Watanabe Y, Nakano T, Yutani K, Nishimura H, Kusuoka H, Nakamura H, Nishimura T. Detection of viable cortical neurons using benzodiazepine receptor imaging after reversible focal ischaemia in rats: comparison with regional cerebral blood flow. *Eur J Nucl Med* 2000; 27:308–313.
12. al-Tikriti MS, Dey HM, Zoghbi SS, Baldwin RM, Zea-Ponce Y, Innis RB. Dual-isotope autoradiographic measurement of regional blood flow and benzodiazepine receptor availability following unilateral middle cerebral artery occlusion. *Eur J Nucl Med* 1994; 21:196–202.
13. Nogawa S, Zhang F, Ross ME, Iadecola C. Cyclo-oxygenase-2 gene expression in neurons contributes to ischemic brain damage. *J Neurosci* 1997; 17:2746–2755.
14. Sairanen T, Ristimaki A, Karjalainen-Lindsberg ML, Paetau A, Kaste M, Lindsberg PJ. Cyclooxygenase-2 is induced globally in infarcted human brain. *Ann Neurol* 1998; 43:738–747.
15. Iadecola C, Forster C, Nogawa S, Clark HB, Ross ME. Cyclooxygenase-2 immunoreactivity in the human brain following cerebral ischemia. *Acta Neuropathol (Berl)* 1999; 98:9–14.
16. Hewett SJ, Uliasz TF, Vidwans AS, Hewett JA. Cyclooxygenase-2 contributes to *N*-methyl-D-asparatate-mediated neuronal cell death in primary cortical cell culture. *J Pharmacol Exp Ther* 2000; 293:417–425.
17. Takedera T, Yumoto H, Tozuka Y, Ohyashiki T. Prostaglandin E(2) induces caspase-dependent apoptosis in rat cortical cells. *Neurosci Lett* 2002; 317:61–64.
18. Gavrieli Y, Sherman Y, Ben-Sasson SA. Identification of programmed cell death in situ via specific labeling of nuclear DNA fragmentation. *J Cell Biol* 1992; 119:493–501.
19. Longa EZ, Weinstein PR, Carlson S, Cummins R. Reversible middle cerebral artery occlusion without craniotomy in rats. *Stroke* 1989; 20:84–91.
20. Minematsu K, Li L, Fisher M, Sotak CH, Davis MA, Fiandaca MS. Diffusion-weighted magnetic resonance imaging:rapid and quantitative detection of focal brain ischemia. *Neurology* 1992; 42:235–240.
21. Kuge Y, Minematsu K, Yamaguchi T, Miyake Y. Nylon monofilament for intraluminal middle cerebral artery occlusion in rats. *Stroke* 1995; 26:1655–1658.
22. Sternberger LA, Sternberger NH. The unlabeled antibody method: comparison of peroxidase- antiperoxidase with avidin-biotin complex by a new method of quantification. *J Histochem Cytochem* 1986; 34:599–605.
23. Tagaya M, Liu K, Copeland B, Seiffert D, Engler R, Garcia JH, Zoppo GJ. DNA scission after focal brain ischemia/temporal differences in two species. *Stroke* 1997; 28:1245–1254.
24. Torizuka K, Uemura K, Toru M, Shinohara Y, Nishimura T, Yonekura Y, Nakagawara J, Matsuda H, Sakai F, Matsuda K, Fukuyama H, Morimoto K. A phase 3 clinical trial of ^{123}I-iomazenil, a new central-type benzodiazepine receptor imaging agent. Part 4. Report on clinical usefulness in diagnosis of cerebrovascular diseases. *Kaku Igaku* 1996; 33:329–344.
25. Moriwaki H, Matsumoto M, Hashikawa K, Oku N, Ishida M, Seike Y, Fukuchi K, Hori M, Nishimura T. Iodine-123-iomazenil and iodine-123-iodoamphetamine SPECT in major cerebral artery occlusive disease. *J Nucl Med* 1998; 39:1348–1353.
26. Matsuoka Y, Okazaki M, Zhao H, Asai S, Ishikawa K, Kitamura Y. Phosphorylation of c-Jun and its localization with heme oxygenase-1 and cyclooxygenase-2 in CA1 pyramidal neurons after transient forebrain ischemia. *J Cereb Blood Flow Metab* 1999; 19:1247–1255.
27. Heiss WD, Grond M, Thiel A, Ghaemi M, Sobesky J, Bauer B, Wienhard K. Permanent cortical damage detected by flumazenil positron emission tomography in acute stroke. *Stroke* 1998; 29:454–461.
28. Heiss WD, Kracht L, Grond M, Rudolf J, Bauer B, Wienhard K, Pawlik G. Early [^{11}C]flumazenil/H_2O positron emission tomography predicts irreversible ischemic cortical damage in stroke patients receiving acute thrombolytic therapy. *Stroke* 2000; 31:366–369.

SHORT REPORT

Isolated pulmonary arteriovenous fistula without Rendu-Osler-Weber disease as a cause of cryptogenic stroke

K Kimura, K Minematsu, M Nakajima

J Neurol Neurosurg Psychiatry 2004;75:311–313

See end of article for authors' affiliations

Correspondence to: Dr K Kimura, Cerebrovascular Division, Department of Medicine, National Cardiovascular Center, 5-7-1 Fujishirodai, Suita, Osaka 565-8565, Japan; kimurak@hsp.ncvc.go.jp

There has been uncertainty as to whether a right to left shunt through an isolated pulmonary arteriovenous fistula (P-AVF) without Rendu-Osler-Weber (ROW) disease can cause paradoxical brain embolism. A population of 747 acute ischaemic stroke patients was examined to determine the frequency and clinical characteristics of those patients who had an isolated P-AVF. The presence of a P-AVF was determined as follows. On patients with a stroke of undetermined cause, both transoesophageal echocardiography and transcranial Doppler with saline contrast medium was performed to detect a right to left shunt. If a P-AVF was then suspected, selective pulmonary angiography and enhanced chest CT was performed to confirm the presence of the P-AVF. Four patients (0.5%) were diagnosed as having a stroke associated with an isolated P-AVF. All the patients were middle-aged women (mean age 61 years). In all these patients, the P-AVF could not have been suspected on physical findings or chest *x* ray. The P-AVF was always single and located in the lower lobe. All the patients had asymptomatic deep venous thrombosis, and three patients developed pulmonary embolism. As D-dimer and thrombin–antithrombin complex were elevated in all patients, this indicated an activation of both fibrinolytic and thrombin activity. Our results show that an isolated P-AVF without ROW disease can cause paradoxical brain embolism. Thus, the existence of an isolated P-AVF as a right to left shunt in patients with a stroke of unknown origin should not be overlooked, even if a P-AVF is not suggested by the initial physical findings or chest *x* ray.

Rendu-Osler-Weber (ROW) disease is characterised by multiple dermal, mucosal, and visceral telangiectasia that are associated with recurrent bleeding, and by a pulmonary arteriovenous fistula (P-AVF) in 15% of patients.[1] The right to left shunt caused by P-AVF with ROW disease can cause paradoxical brain embolism.[1 2] To the best of our knowledge, however, only four cases of paradoxical brain embolism associated with an isolated P-AVF without ROW disease, including our one previous case, have been reported.[3–6] Therefore, the question remains as to whether an isolated P-AVF is associated with ischaemic stroke, and, in particular, with paradoxical brain embolism. The aims of this study were to investigate the frequency of brain infarction associated with an isolated P-AVF, to evaluate the salient clinical characteristics of this condition, and to elucidate a mechanism for the development of ischaemic stroke in these patients.

SUBJECTS AND METHODS

We reviewed the records of 747 consecutive ischaemic stroke patients who were admitted to our division within 7 days of stroke onset between August 1998 and December 2002. We identified those patients with a brain infarction that was associated with an isolated P-AVF without ROW disease. The diagnosis of ROW disease was made clinically based on the "classic triad" of telangiectasia, recurrent epistaxis, and a family history of the disorder. The presence of a P-AVF was determined as follows. When we had a patient with a stroke of undetermined cause, we always performed both a transoesophageal echocardiography (TOE) with saline contrast medium and a transcranial Doppler (TCD) with saline contrast medium so as to detect a right to left shunt, such as a patent foramen ovale (PFO) or a P-AVF. A patient with a stroke of undetermined cause was defined as a patient who did not have a lacunar stroke; did not have more than a 50% stenosis in the cerebral artery irrigating the affected lesions; and had no potential cardiac sources of emboli (such as atrial fibrillation, acute myocardial infarction, old myocardial infarction with intraventricular thrombus, mitral valve disease, prosthetic valve, implantation of a pacemaker, or a dilated cardiomyopathy). If a P-AVF was suspected based on the findings of the TCD study with saline contrast medium that detected microembolic signals (MES) through the middle cerebral artery or the basilar artery, and the TEE did not demonstrate a PFO,[7] we then always performed selective pulmonary angiography and enhanced chest CT so as to confirm the presence of the P-AVF. Pulmonary embolism was diagnosed by lung perfusion scintigraphy, and deep venous thrombosis (DVT) was diagnosed by venography and/or ultrasonography.

RESULTS

ROW disease was not observed in the 747 patients studied. However, seven patients were suspected as having a P-AVF by TCD and TEE studies. Pulmonary angiography and chest CT studies could not confirm a P-AVF in three of these patients. Therefore, four patients (0.5%), including our previously reported patient (case 1),[6] were diagnosed as having an embolic stroke associated with an isolated P-AVF. TCD studies in all these patients showed that MES were detected during normal breathing without having to perform a Valsalva manoeuvre or a cough. The clinical characteristics of all four patients are shown in the table. None of the patients had clinical evidence of hypoxia, such as cyanosis, dyspnea, and erythrocytosis. We could not auscultate vascular sounds in the lung fields, and the chest

Abbreviations: DVT, deep venous thrombosis; MES, microembolic signals; P-AVF, pulmonary arteriovenous fistula; PFO, patent foramen ovale; ROW, Rendu-Osler-Weber; TCD, transcranial Doppler; TOE, transoesophageal echocardiography

Table 1 Clinical characteristics of four patients with P-AVF without Rendu-Osler-Weber disease

	Case 1	Case 2	Case 3	Case 4
Gender	Female	Female	Female	Female
Age (years)	62	59	50	68
Location of brain infarction	Left MCA Territory	Thalamus	Cerebellum	Cerebellum
Medication before stroke onset	–	Ticlopidine (200 mg)	–	Aspirin (80 mg)
History of TIA or brain infarction	+	+	+	+
Risk factor	–	HT, HL	–	HT, HL
Chest *x* ray	Normal	Normal	Normal	Normal
Location of P-AVF in lung	Right lower	Right lower	Right lower	Left lower
Single or multiple P-AVF	Single	Single	Single	Single
Size of P-AVF (mm) on CT	5	7	2	4
DVT	+	+	+	+
Pulmonary embolism	+	+	+	–
RBC count×10 000/μl	377	404	383	327
Hg (g/dL)	11.1	12.0	8.2	10.6
Ht (%)	30.2	38.0	26.8	32.3
PaO_2 (mmHg)	76	85	88	83
TAT μg/L	4.2	3.7	2.7	2.3
D-dimer μg/L	2.4	1.5	3.9	1.1
After embolisation of P-AVF				
Medication	Free	Warfarin	Warfarin	Warfarin
Recurrent stroke	–	–	–	BH
Observation interval (months)	57	45	14	13

MCA, middle cerebral artery; TIA, transient ischaemic attack; HT, hypertension; HL, hyperlipidaemia; BH, brain haemorrhage; TAT, thrombin–antithrombin III complex; P-AVF, pulmonary arteriovenous fistula; DVT, deep venous thrombosis; RBC, red blood cell

x rays did not demonstrate any abnormality, such as a nodular density in the bilateral lung lobes, which would have led us to suspect P-AVF. The P-AVF found on lung CT and pulmonary angiography was always single and located in the lower lobe. The mean size of the P-AVF on CT was 4.5 mm. All patients had pulmonary embolism, and three had asymptomatic deep venous thrombosis. D-dimer and thrombin–antithrombin complex were elevated in all patients, indicating the activation of both fibrinolytic and thrombin activity.

The P-AVFs were occluded with catheter embolisation within 2 months of stroke onset. Our follow up was conducted for an average of 32 months (range 13–57 months), and no recurrent ischaemic strokes were documented, but one patient (case 4) had a thalamic haemorrhage 8 months after catheter embolisation of the P-AVF. This patient had been treated with warfarin and her international normalised ratio was 2.2 at the onset of the brain haemorrhage.

Fig 1 shows the findings of case 2: a pulmonary angiography with a P-AVF; a venogram of the lower limbs showing a DVT; and lung perfusion scintigraphy showing pulmonary embolism.

DISCUSSION

We have presented four acute ischaemic stroke patients with P-AVF not associated with ROW disease. None of the patients had cardiac or arterial sources for the emboli. Furthermore, all the patients had DVTs and three patients developed pulmonary embolism. Therefore, we diagnosed all these patients as having had paradoxical brain embolism through a P-AVF. We conclude that an isolated P-AVF can cause paradoxical brain embolism.

It is of interest to note that the size of the P-AVFs differed between previously reported cases and our patients. The previously reported cases, due to the large size of the P-AVFs,[3–5] had physical findings, such as auscultate vascular sounds, or abnormalities on chest *x* ray. In contrast, in all of our patients the P-AVFs could not be suspected on physical findings or chest *x* ray, because of their small size. Therefore, the presence of P-AVF in stroke patients who have normal physical findings and no chest *x* ray abnormalities cannot be excluded.

A TCD with saline contrast medium performed on all patients was useful in identifying the presence of a P-AVF during the acute phase of the stroke. As a persistent right to left shunt occurs in a P-AVF, micro air bubbles can be detected in the cerebral arteries using TCD with saline contrast medium during normal breathing without the need to use provocative methods, such as a Valsalva manoeuvre or a cough.[7] Therefore, in patients who have had an embolic

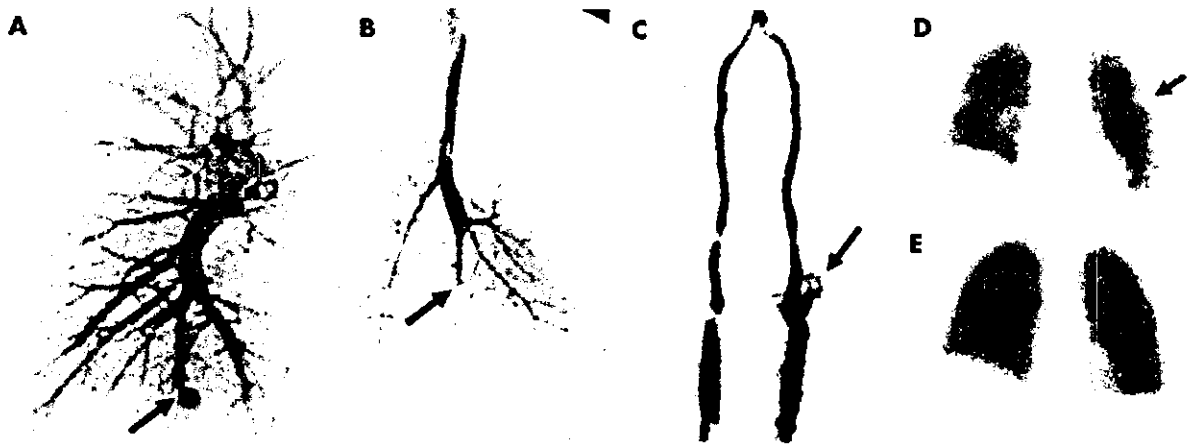

Figure 1 The pulmonary angiography (A, B), venogram of the lower limbs (C), and the ventilation–perfusion lung scintigraphy (D, E) of case 2. (A) Selective pulmonary angiography 30 days after stroke onset shows a P-AVF (arrow) in the right lower lobe. (B) After embolisation therapy with a metal coil, the feeding vessels to the P-AVF are completely occluded. (C) Venogram of the left lower limbs 4 days after stroke onset shows the abnormal collateral flow (arrow) in the leg veins, indicating a deep venous thrombus. (D) Lung perfusion scintigram 4 days after stroke onset shows the defect (arrow) in the left upper lung, indicating a pulmonary embolism. (E) The follow-up study taken 24 days after stroke onset shows no perfusion defect in the left upper lung.

stroke of undetermined cause and cannot perform a Valsalva manoeuvrer or a cough because of aphasia or a disturbance of consciousness, TCD with saline contrast medium can help detect a P-AVF in the acute phase of stroke.

Catheter embolisation is a safe and effective treatment for P-AVF.[8] All four patients had a history of ischaemic stroke or TIA prior to the present stroke. After catheter embolisation of their P-AVF, none of these patients had a recurrent ischaemic stroke. Thus, catheter embolisation of a P-AVF appears to be an effective method of preventing recurrent ischaemic stroke in such patients.

In conclusion, an isolated P-AVF without ROW disease can cause cryptogenic stroke. Thus, one should not overlook an isolated P-AVF as a right to left shunt in patients with a stroke of unknown origin, even when physical findings or chest *x* ray findings are not suggestive of a P-AVF.

ACKNOWLEDGEMENTS

This study was supported in part by Research Grants for Cardiovascular Disease (12A-4, 14C-1) from the Ministry of Health, Labor and Welfare of Japan.

Authors' affiliations
K Kimura, K Minematsu, M Nakajima, Cerebrovascular Division, Department of Medicine, National Cardiovascular Center, Fujishirodai, Suita, Osaka, Japan

Competing interest: none declared

REFERENCES

1 **Peery WH.** Clinical spectrum of hereditary hemorrhagic telangiectasia (Osler-Weber-Rendu Disease). *Am J Med* 1986;**82**:989–97.
2 **Moussouttas M,** Fayad P, Rosenblatt M, *et al.* Pulmonary arteriovenous malformations: cerebral ischemia and neurologic manifestations. *Neurology* 2000;**55**:959–64.
3 **Reguera JM,** Colmenero JD, Gurrero M, *et al.* Paradoxical cerebral embolism secondary to pulmonary arteriovenous fistula. *Stroke* 1990;**21**:504–5.
4 **Geyskens W,** Dymarkowski S, Budts W, *et al.* Quiz case of the month. *Eur Radiol* 2000;**10**:1997–8.
5 **Puskas JD,** Allen MS, Moncure AC, *et al.* Pulmonary arteriovenous malformations: Therapeutic options. *Ann Thorac Surg* 1993;**56**:253–8.
6 **Kimura K,** Minematsu K, Wada K, *et al.* Transcranial Doppler of a paradoxical brain embolism associated with a pulmonary arteriovenous fistula. *AJNR Am J Neuroradiol* 1999;**20**:1881–4.
7 **Chimowitz MI,** Nemec JJ, Marwick TH, *et al.* Transcranial Doppler ultrasound identifies patients with right-to-left cardiac or pulmonary shunts. *Neurology* 1991;**41**:1902–4.
8 **Lee DW,** White RI, Egglin TK, *et al.* Embolotherapy of large pulmonary arteriovenous malformations: Long-term results. *Ann Thorac surg* 1997;**64**:930–40.

ELSEVIER

Neuroscience Letters 357 (2004) 219–222

Neuroscience Letters

www.elsevier.com/locate/neulet

Temporal and topographic profiles of cyclooxygenase-2 expression during 24 h of focal brain ischemia in rats

Chiaki Yokota[a,*], Tomohito Kaji[b], Yuji Kuge[c], Hiroyasu Inoue[d], Nagara Tamaki[b], Kazuo Minematsu[e]

[a]*Cerebrovascular Laboratory, Department of Pathogenesis, National Cardiovascular Center Research Institute, 5-7-1 Fujishirodai, Suita, Osaka, 565-8565, Japan*
[b]*Department of Nuclear Medicine, Graduate School of Medicine, Hokkaido University, Sapporo, Japan*
[c]*Department of Patho-functional Bioanalysis, Graduate School of Pharmaceutical Sciences, Kyoto University, Kyoto, Japan*
[d]*Division of Molecular Pharmacology, Department of Pharmacology, National Cardiovascular Center Research Institute, Osaka, Japan*
[e]*Cerebrovascular Division, Department of Medicine, National Cardiovascular Center, Osaka, Japan*

Received 6 October 2003; received in revised form 17 December 2003; accepted 26 December 2003

Abstract

Substantial increases in cyclooxygenase-2 (COX-2) mRNA and protein levels were demonstrated in the peri-infarct and focal ischemic areas after 3–24 and 12–24 h, respectively, in rats. In the ischemic core, significant increases in COX-2 mRNA followed 6 h of ischemia, though the peak level was about one-third of that in the peri-infarct area. Increases in COX-2 protein in the ischemic core were not observed during ischemic periods. Diffuse, neuronal COX-2 staining was found in peri-infarct areas as well as in discrete, immunoreactive neurons in the ischemic core. Robust increases in prostaglandin E_2 levels in the peri-infarct area were demonstrated following 24 h of ischemia. Prostaglandin production as well as COX-2 expression in ischemic tissues depended on the degree and duration of the reduction in cerebral blood flow.

Keywords: Cyclooxygenase-2; Focal brain ischemia; Prostaglandin E_2; 6-keto-PG $F_{1\alpha}$; Cerebral blood flow; Rat

Cyclooxygenase-2 (COX-2), a rate-limiting enzyme in prostaglandin synthesis, is rapidly induced by proinflammatory cytokines in vitro and has been shown to mediate the induction of prostaglandin synthesis during the inflammatory response in vivo [17]. Accumulating evidence suggests that inflammatory processes play a role in the development and progression of atherosclerosis [2,8,14] and COX-2 in particular has become the focus of attention as a therapeutic target enzyme in acute coronary syndromes [1] and Alzheimer's disease [16]. We previously reported that neuronal COX-2 was induced within potentially viable hypoperfused brain areas after a 24 h ischemic period in non-human primates [20]. The role of neuronal COX-2 within such peri-infarct areas, however, is still unclear. Several reports using various rodent models suggested that COX-2 played a role in the development of ischemic injury [3,4,12]. A few postmortem reports suggested that the production of prostanoids by COX-2 after acute ischemia could contribute to the remodeling of neural networks that is seen after focal infarction [15]. The objective of the present study was to elucidate the topography and time course of COX-2 expression and prostaglandin (PG) E_2 (the major prostanoid involved in inflammation) production, as well as the production of the prostacyclin metabolite 6-keto-PG $F_{1\alpha}$ [11,13] during 24 h of focal brain ischemia.

Male Sprague–Dawley rats (300–350 g, $n = 40$) were used in this study. All procedures were approved by our Institutional Animal Research Committee and were performed in accordance with the standards published by the National Research Council. Rats were anesthetized with chloral hydrate (400 mg/kg body weight i.p.) and focal brain ischemia was produced by the intraluminal occlusion of the ostium of the right middle cerebral artery with nylon monofilaments, as previously described [7,9]. Rectal temperatures were monitored and maintained at around 37

* Corresponding author. Tel.: +81-6-6833-5012; fax: +81-6-6872-8091.
E-mail address: cyokota@ri.ncvc.go.jp (C. Yokota).

0304-3940/03/$ - see front matter © 2003 Elsevier Ireland Ltd. All rights reserved.
doi:10.1016/j.neulet.2003.12.109

°C with the aid of heating pads. Rats were sacrificed under chloral hydrate anesthesia at time 0 and at different times points after arterial occlusion (1, 2, 3, 4, 6, 8, 12, and 24 h, $n = 4$-5/time point) and their brains immediately immersed in ice-cold saline. The brains were then cut into four coronal sections (blocks A–D) as shown in Fig. 1A. Several blocks were frozen in isopentane-dry ice and stored at −80 °C until use, whereas others (from C) were embedded in paraffin for immunohistochemistry. Analysis of COX-2 expression (mRNA, protein), and measurement of the concentrations of PGE_2 and the prostacyclin metabolite 6-keto-PG $F_{1\alpha}$ in the peri-infarct areas and the ischemic core were performed using blocks A and C, respectively.

In some animals, *N*-isoproryl-*p*-[^{125}I]-iodoamphetamine ([^{125}I]IMP) (2.22 MBq/kg body weight) was injected into the femoral vein 5 min before sacrifice and ex vivo autoradiography was performed to measure cerebral blood flow (CBF) using blocks B and D. For each frozen block, tissues that were adjacent to block C were serially sectioned (20 μm). Exposure was carried out for 7 days in order to visualize the distribution of [^{125}I]IMP. The autoradiograms were analyzed using a computerized imaging analysis system (Bio-imaging Analyzer BAS-5000, Fuji Photo Film, Tokyo, Japan). A total of four regions of interest (ROIs), as shown in Fig. 1B, were bilaterally and symmetrically positioned in the cerebral cortices in each coronal slice of blocks B and D. Asymmetry indices (AIs) were defined as the ratios of values for ROIs in the hemisphere ipsilateral to the arterial occlusion (right) to those of the contralateral homologous ROIs. AIs of the ischemic core were defined as a/d, whereas the AIs of the peri-infarct area were defined as b/c (Fig. 1B). An average AI value from blocks B and D was calculated for the CBF in each area of the ischemic core and peri-infarction areas.

RNA preparation and blot analysis were performed using cortices from blocks A (peri-infarct area) and C (ischemic core) as previously described [6]. For the immunoblot analyses, right cortical samples from block A (peri-infarct area) were obtained from each animal at time 0, and 3, 6, 12, and 24 h after ischemia ($n = 4$-5 for each period). The sample volumes, which were about 20 mg for each animal, were pooled together for each ischemic period. Right

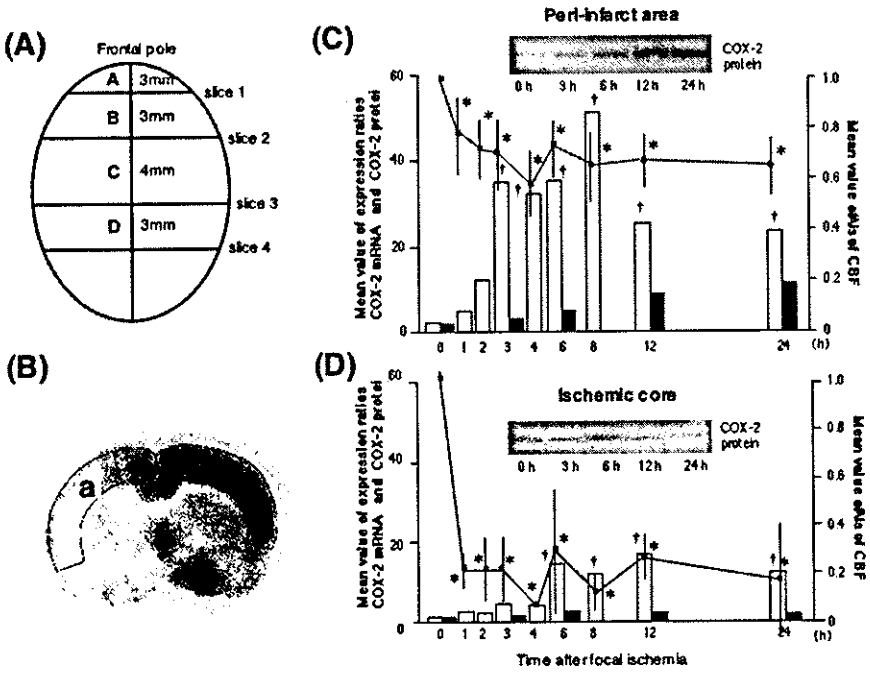

Fig. 1. Temporal profile of COX-2 expression associated with changes in CBF during 24 h of ischemia. (A) The brain was stereotaxically divided, on ice, into four coronal sections using a brain matrix. The first slice was made 3 mm from the frontal pole (block A), while the other three were cut at 3 mm (block B), 7 mm (block C), and 10 mm (block D) intervals posterior to the first slice. Determination of COX-2 expression levels (mRNA, protein) in the peri-infarct area and ischemic core was performed using blocks A and C, respectively. (B) To measure CBF in each animal, four regions of interest (ROIs) were bilaterally symmetrically placed on the cerebral cortices using coronal frozen slices from blocks B and D. Asymmetry indices (AIs) of the ischemic core were defined as a/d, whereas the AIs of the peri-infarct area were defined as b/c. (C,D) Lines indicate the mean AI values of CBF. The open and solid columns correspond to the mean expression ratios of COX-2 mRNA and COX-2 protein, respectively. Figures C and D show the time course of COX-2 expression in the peri-infarct area and ischemic core, respectively. A one-way ANOVA and post-hoc Fisher's tests were used to assess the differences in AIs and expression ratios of COX-2 mRNA between the different ischemic time points. CBF values in the peri-infarct area and ischemic core were significantly reduced compared to controls immediately after arterial occlusion ($^*P < 0.05$). The mean CBF values in the ischemic core and peri-infarct area were 0.19 ± 0.07 (mean ± SD) and 0.67 ± 0.06, respectively. The time course of COX-2 expression in the peri-infarct area was different from that in the ischemic core. Thus, the expression ratios of COX-2 mRNA increased significantly after 3 h of ischemia ($^\dagger P < 0.05$), with COX-2 protein also increasing with time in the peri-infarct area. On the other hand, significant increases in COX-2 mRNA were found 6 h after ischemia ($^\dagger P < 0.05$), and increases in COX-2 protein were not observed during the ischemic period in the ischemic core.

cortical samples from block C (ischemic core) for each ischemic period were also pooled together in this manner. Immunoblot analyses were then performed on each pooled sample as previously described [19]. COX-2 expression (mRNA, protein) in the ischemic cortices was calculated as expression ratios, defined as the ratio of the COX-2 mRNA or protein signals in the ischemic samples to their mean values in the corresponding control areas.

For immunohistochemistry, a mirror sectioning technique was used to colocalize COX-2 and microtubule-associated protein 2 (MAP-2), a neuronal skeletal protein, in sections from block C as previously described [19]. Negative controls consisted of sections that were incubated overnight without the primary antibody and processed as above.

Tissue concentrations of PGE_2 and 6-keto-PG $F_{1\alpha}$ in the right (ischemic) cortices of blocks A (peri-infarct area) and C (ischemic core) were determined using radioimmunoassay kits (Perkin-Elmer Life Sciences, Inc. MA, USA), and values were normalized for protein content.

Significant reductions in AIs for CBF in the peri-infarct area and ischemic core were demonstrated in animals at each ischemic time point compared to controls (Fig. 1C,D). The expression ratios of COX-2 mRNA increased significantly between 3 and 24 h of ischemia in the peri-infarct area compared to controls (Fig. 1C). In the ischemic core, significant increases in COX-2 mRNA were seen following 6 h of ischemia, which remained through 24 h (Fig. 1D). The peak value of the expression ratio of COX-2 protein in the peri-infarct area was 10.7 at 24 h of ischemia, while the peak expression ratio in the ischemic core was 2.0 at 6 h of ischemia.

COX-2 immunoreactive neurons were found predominantly in the peri-infarct area, though elevations in the immunohistochemical staining of discrete neuronal populations were also observed in the ischemic core (Fig. 2). Both COX-2 and MAP-2 immunoreactivity were abolished when the primary antibody was omitted.

Although no significant increases in PGE_2 and prostacyclin levels were observed in the peri-infarct and ischemic core areas following 3 h of ischemia, significant increases in prostaglandin levels were found in the ischemic hemisphere

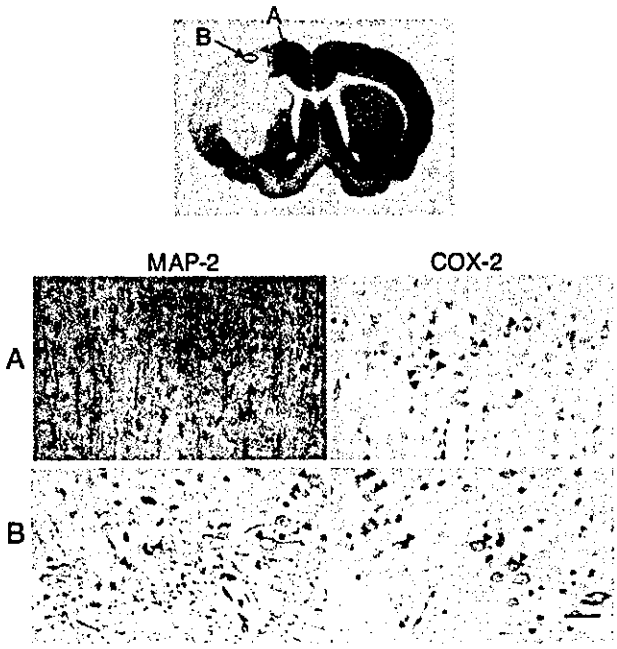

Fig. 2. Immunohistochemical analysis of COX-2. The single top figure shows a coronal slice of the brain of an animal that had undergone 3 h of ischemia, which was immunostained for microtubule-associated protein 2 (MAP-2). The bottom figures are sections that were immunostained for COX-2 and MAP-2 that were derived from either the peri-infarct area (region A in the top figure) or the ischemic core (B). Immunoreactive COX-2 and MAP-2 were localized in the same neurons in the ischemic core and peri-infarct area (arrow heads). Scale bar: 100 μm.

following 24 h of ischemia. In particular, PGE_2 levels in the peri-infarct area increased significantly (Table 1).

We previously demonstrated, in a small number of non-human primates, that post-ischemic COX-2 expression was regulated by the extent of CBF reduction [20]. In the present study, serial changes in the expression of COX-2 during focal ischemia were evaluated more closely in relation to the degree and duration of CBF reduction, and COX-2 reaction products (PGE_2 and prostacyclin), which were not analyzed in our previous study, were also examined. The time course of COX-2 expression in the ischemic core, characterized by a CBF of $<20\%$ of baseline values, was different from that seen in the peri-infarct area, where 70–80% of control CBF was observed following 24 h of ischemia. The upregulation

Table 1
Prostaglandin production (pg/mg total protein) in the right (ischemic) hemisphere

Prostaglandin	Duration of ischemia (h)	Peri-infarct area	Ischemic core
PGE_2	0	60.8 ± 16.6	21.4 ± 11.4
	3	156.6 ± 70.1	54.4 ± 22.3
	24	2609.0 ± 2522.0*†	414.6 ± 226.3*†
Prostacyclin metabolite (6-keto-PG $F_{1\alpha}$)	0	122.3 ± 47.6	47.6 ± 23.0
	3	200.8 ± 59.7	93.4 ± 43.5
	24	1143.0 ± 623.7*†	341.6 ± 84.5*†

*$P < 0.05$ vs. 0 h (control); †$P < 0.05$ vs. 3 h ischemia by ANOVA. The values are the mean ± SD.

of COX-2 mRNA in the peri-infarct area persisted for at least 24 h after ischemia, as did the production of COX-2 protein, which led to significant increases in prostacyclin as well as PGE_2 levels following 24 h of ischemia. In the ischemic core, increases in COX-2 mRNA persisted during the 24 h of ischemia, though significant increases in COX-2 protein were not observed. This latter finding was considered to be due to the severe ischemic injury that was caused by reduced CBF, which likely affected protein synthesis [5]. This assertion is supported by the work of Xie et al. [18] who reported that a CBF of <70% of controls suppressed protein synthesis. In spite of these effects on COX-2 protein, significant increases were seen in the concentration of prostaglandins in the ischemic core 24 h after ischemia. Local increases in neuronal COX-2 expression in the ischemic core, as determined by immunohistochemical analysis, could have accounted for this increase in prostaglandin concentration. Increases in PGE_2 in ischemic cortices after 24 h of ischemia, particularly in peri-infarct areas, were probably due to the upregulation of membrane-associated PGE_2 synthase (mPGES) activity as well as the induction of COX-2, which were reported to be essential components for delayed PGE_2 biosynthesis [10].

The induction of neuronal COX-2 is important for the regulation of prostaglandin signaling in post-ischemic regions, and the magnitude of COX-2 activity and prostaglandin production is determined by the degree and duration of CBF reduction. Before novel therapeutic options for stroke patients can be developed, further clarification of the effects of COX-2 during and after ischemia will be required.

Acknowledgements

This study was supported in part by a Grant-in-Aid for Scientific Research from the Japan Society for the Promotion of Science, by grants from the Takeda Medical Research Foundation, by the Mitsubishi Pharma Research Foundation, and by the Japan Heart Foundation.

References

[1] R. Altman, H.L. Luciardi, J. Muntaner, F.D. Rio, S.G. Berman, R. Lopez, C. Gonzalez, Efficacy assessment of meloxicam, a preferential cyclooxygenase-2 inhibitor, in acute coronary syndromes without ST-segment elevation: the Nonsteroidal Anti-Inflammatory Drugs in Unstable Angina Treatment-2 (NUT-2) pilot study, Circulation 106 (2002) 191–195.

[2] F.C. Barone, G.Z. Feuerstein, Inflammatory mediators and stroke: new opportunities for novel therapeutics, J. Cereb. Blood Flow Metab. 19 (1999) 819–834.

[3] Y. Collaco-Moraes, B. Aspey, M. Harrison, J. de-Belleroche, Cyclo-oxygenase-2 messenger RNA induction in focal cerebral ischemia, J. Cereb. Blood Flow Metab. 16 (1996) 1366–1372.

[4] K. Hara, D.L. Kong, F.R. Sharp, P.R. Weinstein, Effect of selective inhibition of cyclooxygenase 2 on temporary focal cerebral ischemia in rats, Neurosci. Lett. 256 (1998) 53–56.

[5] K.A. Hossmann, Viability thresholds and the penumbra of focal ischemia, Ann. Neurol. 36 (1994) 557–565.

[6] H. Inoue, C. Yokoyama, S. Hara, Y. Tone, T. Tanabe, Transcriptional regulation of human prostaglandin-endoperoxide synthase-2 gene by lipopolysaccharide and phorbol ester in vascular endothelial cells, J. Biol. Chem. 270 (1995) 24965–24971.

[7] Y. Kuge, K. Minematsu, T. Yamaguchi, Y. Miyake, Nylon monofilament for intraluminal middle cerebral artery occlusion in rats, Stroke 26 (1995) 1655–1658.

[8] P.L. McGeer, M. Schulzer, E.G. McGeer, Arthritis and anti-inflammatory agents as possible protective factors for Alzheimer's disease: a review of 17 epidemiologic studies, Neurology 47 (1996) 425–432.

[9] K. Minematsu, L. Li, M. Fisher, C.H. Sotak, M.A. Davis, M.S. Fiandaca, Diffusion weighted magnetic resonance imaging: rapid and quantitative detection of focal brain ischemia, Neurology 42 (1992) 235–240.

[10] M. Murakami, H. Naraba, T. Tanioka, N. Semmyo, Y. Nakatani, F. Kojima, T. Ikeda, M. Fueki, A. Ueno, S. Oh-ishi, I. Kudo, Regulation of prostaglandin E2 biosynthesis by inducible membrane-associated prostaglandin E2 synthase that acts in concert with cyclooxygenase-2, J. Biol. Chem. 275 (2000) 32783–32792.

[11] T. Murata, F. Ushikubi, T. Matsuoka, M. Hirata, A. Yamasaki, Y. Sugimoto, A. Ichikawa, Y. Aze, T. Tanaka, N. Yoshida, A. Ueno, S. Oh-ishi, S. Narumiya, Altered pain perception and inflammatory response in mice lacking prostacyclin receptor, Nature 388 (1997) 678–682.

[12] S. Nogawa, F. Zhang, M.E. Ross, C. Iadecola, Cyclo-oxygenase-2 gene expression in neurons contributes to ischemic brain damage, J. Neurosci. 17 (1997) 2746–2755.

[13] J.P. Portanova, Y. Zhang, G.D. Anderson, D.D. Hauser, J.L. Masferrer, K. Seibert, S.A. Gregory, P.C. Isakson, Selective neutralization of prostaglandin E2 blocks inflammation, hyperalgesia, and interleukin 6 production in vivo, J. Exp. Med. 184 (1996) 883–891.

[14] R. Ross, Atherosclerosis – an inflammatory disease, N. Engl. J. Med. 340 (1999) 115–126.

[15] T. Sairanen, A. Ristimaki, M.-L. Karjalainen-Lindsberg, A. Paetau, M. Kaste, P.J. Lindsberg, Cyclooxygenase-2 induced globally in infarcted human brain, Ann. Neurol. 43 (1998) 738–747.

[16] C. Scali, M.G. Giovannini, C. Prosperi, A. Bellucci, G. Pepeu, F. Casamenti, The selective cyclooxygenase-2 inhibitor rofecoxib suppresses brain inflammation and protects cholinergic neurons from excitotoxic degeneration in vivo, Neuroscience 117 (2003) 909–919.

[17] D.A. Willoughby, A.R. Moore, P.R. Colville-Nash, COX-1, COX-2, and COX-3 and the future treatment of chronic inflammatory disease, Lancet 355 (2000) 646–648.

[18] Y. Xie, G. Mies, K.A. Hossmann, Ischemic threshold of brain protein synthesis after unilateral carotid artery occlusion in gerbils, Stroke 20 (1989) 620–626.

[19] C. Yokota, H. Inoue, Y. Kuge, T. Abumiya, M. Tagaya, Y. Hasegawa, N. Ejima, N. Tamaki, K. Minematsu, Cyclooxygenase-2 expression associated with spreading depression in a primate model, J. Cereb. Blood Flow Metab. 23 (2003) 395–398.

[20] C. Yokota, Y. Kuge, H. Inoue, M. Tagaya, G. Kito, T. Susumu, N. Tamaki, K. Minematsu, Post-ischemic cyclooxygenase-2 expression is regulated by the extent of cerebral blood flow reduction in non-human primates, Neurosci. Lett. 341 (2003) 37–40.

Original Paper

Cerebrovascular Diseases

Cerebrovasc Dis 2004;18:111–116
DOI: 10.1159/000079258

Received: June 2, 2003
Accepted: January 14, 2004
Published online: June 22, 2004

Long-Term Prognosis, by Stroke Subtypes, after a First-Ever Stroke: A Hospital-Based Study over a 20-Year Period

Chiaki Yokota[a,b] Kazuo Minematsu[b] Yasuhiro Hasegawa[b]
Takenori Yamaguchi[b]

[a]Cerebrovascular Laboratory, National Cardiovascular Center Research Institute, and [b]Cerebrovascular Division, Department of Medicine, National Cardiovascular Center, Osaka, Japan

Key Words
Stroke recurrence · Recurrence-free survival · Risk factors · Japan

Abstract
Background and Purpose: The influence of stroke subtype on recurrence, and determinants of recurrence-free survival after a first-ever stroke are not fully understood. We aimed to clarify the long-term prognosis by stroke subtypes and to identify determinants for recurrence and death after a first-ever stroke. ***Methods:*** We enrolled 1,732 consecutive patients (men/women = 1,134/598, mean age of 65 years) with a first-ever acute stroke who were admitted to our Stroke Care Unit during a period of 20 years. Stroke subtypes were classified as atherothrombotic brain infarction, lacunar infarction, cardioembolic infarction, other type of infarction, and brain hemorrhage. The prognosis was assessed by stroke subtypes. ***Results:*** During the hospital stay (mean 61 days), 99 patients died: 73 died directly from stroke. A total of 198 patients had recurrent strokes, and 286 died within 3 years after the index stroke. The overall recurrence rate within the first year was 6.5%, which was different among stroke subtypes. Patients with cardioembolic infarction (9.0%) as well as other type of infarction (9.1%) had more recurrent strokes within the initial year compared with the other subtypes. A history of transient ischemic attack (relative risk = 1.38), atrial fibrillation (1.52), ischemic heart disease (1.40), and disability at discharge (2.64) were independent predictors for the recurrence and death within 3 years after the first-ever stroke. ***Conclusions:*** The recurrence rate was different among stroke subtypes within 1 year after the index stroke. Atrial fibrillation, ischemic heart disease, history of transient ischemic attack, and disability at discharge were important determinants for stroke recurrence and death.

Introduction

Stroke is a major cause of death and disability throughout the world. In Japan, stroke was the third leading cause of death after cancer and heart disease in 2000. Although stroke mortality in Japan has declined markedly since 1970 [1], the actual number of stroke patients has been increasing along with a rapid increase in the elderly population. As acute stroke events and disability among stroke survivors produce a great burden to the social and health care systems, the prevention and better treatment of stroke have a considerable public health significance. Un-

KARGER
Fax + 41 61 306 12 34
E-Mail karger@karger.ch
www.karger.com

1015–9770/04/0182–0111$21.00/0

Accessible online at:
www.karger.com/ced

Chiaki Yokota, MD
Cerebrovascular Laboratory, National Cardiovascular Center Research Institute
5-7-1 Fujishirodai, Suita, Osaka, 565-8565 (Japan)
Tel. +81 6 6833 5012, Fax +81 6 6872 8091
E-Mail cyokota@ri.ncvc.go.jp

derstanding the considerable heterogeneity in risk factors, stroke incidence, and mortality among different geographic and ethnic populations is important for advancing available prevention strategies for stroke in the world. However, little is known about the long-term outcome by stroke subtypes in Asians.

Our hospital, National Cardiovascular Center, is located in the second largest urban area (Osaka) in Japan. A Stroke Care Unit for acute stroke patients has been operating since 1978. The aim of this study was to determine whether stroke recurrence and mortality are different among stroke subtypes, and to determine whether conventional stroke risk factors and disability at discharge influenced recurrence-free survival after a first-ever stroke.

Subjects and Methods

Subjects

Out of 2,192 patients admitted to the Stroke Care Unit within 7 days of complete stroke onset from April 1, 1978 to March 31, 1997, 1,732 consecutive patients (1,134 men and 598 women, 12–96 years) with a first-ever stroke were enrolled in the present study. Patients with aneurysmal subarachnoid hemorrhages were not included.

Baseline Assessment

Baseline clinical characteristics were recorded, including age, sex, hypertension (HT), hyperlipidemia (HLP), diabetes mellitus (DM), ischemic heart disease (IHD), history of transient ischemic attack (TIA), and atrial fibrillation (AF). The information about conventional risk factors and past medical history were obtained from the hospital records (all medical records are being kept permanently in our hospital), or were inferred from a self-reported medical history or prescribed medication. HLP was defined as a total cholesterol level of >220 mg/dl or triglyceride level of >140 mg/dl, and HT was assessed from systolic blood pressure ≥140 mm Hg, or diastolic pressure ≥90 mm Hg at two independent measurements 2 weeks after stroke onset. DM was defined as a fasting blood glucose level ≥140 mg/dl, or ambient blood glucose ≥ 200 mg/dl after the initial 14 days. Patients who had been treated with insulin or oral hypoglycemic agents were also defined as diabetics. AF was diagnosed by electrocardiography, including 24-hour monitoring, during the hospital stay.

A baseline assessment was performed on every patient: brain CT, carotid ultrasonography (including Dopscan), electrocardiography, as well as standard blood and urine tests. In order to evaluate cerebral arteries, 63% of patients received the conventional cerebral angiography and 8% underwent magnetic resonance angiography in addition to the carotid ultrasonography. Two-dimensional echocardiography was performed on 353 patients with possible cardioembolic infarction to investigate a potential embolic source.

Diagnosis of Stroke Subtypes

The diagnosis of stroke subtypes, such as atherothrombotic brain infarction (ABI), lacunar infarction (LI), cardioembolic infarction (CEI), other type of infarction (OTI), and brain hemorrhage (BH), was made by taking into account all the available data described above, mainly according to the criteria in the Classification of Cerebrovascular Disease III [2].

A diagnosis of ABI was based on the presence of focal brain infarct(s) in the collection of evidence for occlusive lesions in the large cervical and intracranial arteries (either occlusion, ≥50% stenosis of the lumen diameter, or ulceration). In patients with ABI, the responsible vascular lesion for the index stroke was determined by the clinical data. The diagnosis of LI was made when a typical clinical syndrome was associated with a small infarct, ≤15 mm in diameter on CT, restricted to the territory of a perforating artery, and when no evidence of adjacent major artery occlusion or severe stenosis was found [3]. CEI was clinically diagnosed as described elsewhere [4]. If the patient had a combination of the above etiologies, or if the stroke had other causes, such as arterial dissection, cerebral venous thrombosis, or had undetermined etiologies, the index stroke was categorized as OTI. The diagnosis of BH was based on CT findings.

Patient Outcome and Medical Treatment at Discharge

Patient outcome at discharge was assessed with the modified Rankin Scale score [5], trichotomized to good (0–2), poor (3–5), or death. Patients who survived the initial hospitalization were defined as stroke survivors. Any uses of warfarin or antiplatelet agents at discharge were also noted.

Patient Follow-Up

Every effort was made to have in-person follow-up for a period of at least 3 years after the index stroke. The end point events of death or recurrent stroke, defined as a new neurological deficit fitting the definitions for ischemic or hemorrhage stroke, were assessed and recorded by experienced stroke physicians. The follow-up continued until March 31, 2000 or until the end point. Eighty-three percent (1,429 patients) were followed up completely for at least 3 years after the index stroke, or until the end point events. Postal surveys were conducted to identify recurrence or death for the remaining subjects, who moved out of the area or stopped visiting our outpatient clinic after their discharge, making it impossible to pinpoint the occurrence of their end point events within 3 years after the index stroke. In cases of death, medical records and death certificates were reviewed to determine causes of death.

Statistical Analysis

To evaluate changes in clinical characteristics during the 20-year study period, we performed subanalyses by the time trends, and by the two age groups. In the analysis by the time trends, subjects were divided into two groups: patients who were admitted in the initial decade (n = 894) and those admitted in the recent decade (n = 838). In the analyses by the two age groups, we compared patients who were 64 years or younger (younger group; mean age of 54 years, n = 821) with those who were 65 years or older (older group; mean age of 74 years, n = 911).

Statistics were performed using the SPSS package for Macintosh. The baseline clinical characteristics were assessed in a total of 1,732 patients. To determine the differences in clinical backgrounds among stroke subtypes, the χ^2 test, Student's t test, Fisher exact test, or one-way analysis of variance with a Scheffe's post hoc test were used as appropriate.

Table 1. Clinical characteristics of 1,732 patients with different subtypes of stroke

Characteristics	ABI	LI	CEI	OTI	BH	p
Cases	287 (17)	556 (32)	371 (21)	168 (10)	350 (20)	n.s.
Male	216	387	207	103	220	
Female	71	169	164	65	130	
Age (mean ± SD), years	67 ± 10	66 ± 11	64 ± 13	64 ± 16	61 ± 13	<0.05
History of TIA	60 (21)	82 (15)	33 (9)	25 (7)	4 (2)	<0.05
HT	244 (85)	417 (75)	127 (34)	98 (58)	284 (81)	<0.05
DM	103 (36)	149 (27)	67 (18)	40 (24)	56 (16)	<0.05
HLP	123 (43)	180 (32)	91 (25)	52 (31)	108 (31)	<0.05
IHD	53 (19)	51 (9)	54 (15)	29 (17)	16 (5)	<0.05
AF	19 (7)	24 (4)	287 (77)	19 (11)	12 (3)	<0.05
Hospital stay (mean ± SD), days	72 ± 45	43 ± 24	76 ± 58	63 ± 54	66 ± 51	<0.05

Figures in parentheses indicate percentages.

We analyzed long-term prognosis within 3 years after the index stroke. We excluded 167 patients (9.6%) from the analyses who provided no information about their outcome within 3 years after the index stroke in spite of postal surveys. Recurrence-free survival time for stroke survivors was calculated from the date of discharge. Recurrence-free survival rate by stroke subtypes was analyzed by the Kaplan-Meier method. Reasons for censoring included surgical operations, such as extracranial-intracranial bypass surgery and carotid endarterectomy, as well as subject dropout. The log-rank test was used to compare recurrence-free survival rates among stroke subtypes. We estimated the independent contribution of each risk factor to the risk of stroke recurrence or death within 3 years after the index stroke by Cox proportional hazard models. For all statistical analyses, a value of $p < 0.05$ was considered to indicate significant difference.

Results

Clinical Characteristics

Clinical characteristics were compared by stroke subtypes (table 1). Cardiac sources of emboli in 371 patients with CEI were as follows: nonvalvular AF in 144 patients (40%), rheumatic heart disease in 94 (25%), prosthetic valve in 38 (10%), dilated cardiomyopathy in 38 (10%), sick sinus syndrome or pacemaker implantation in 27 (7%), and others in 30 (8%). Two hundred and one patients with ABI (70%) had significant stenosis in the carotid system. Thirty-seven patients had ABI with carotid lesions (18%) associated with IHD: 31 patients had extracranial and 6 had intracranial lesions. In patients with BH, 223 patients (64%) had basal ganglionic, 26 (7%) had pontine, 13 (4%) had cerebellar, 55 (16%) had lobar, and the remaining (n = 33, 9%) had unclassified hematomas.

The distribution of stroke subtypes in the recent decade was significantly different from that in the initial decade. The frequency of patients with LI increased in the recent decade compared with that in the initial decade (35 vs. 29%), while the frequency of BH decreased in the recent decade (16 vs. 25%). The proportion of patients with ABI whose responsible vascular lesion was extracranial had increased significantly in the recent decade (63 vs. 40%). The duration of hospital stay became shorter in the second decade (median 42 days) than it was in the first decade (median 53 days). The proportion of stroke subtypes was also different in the age groups, particularly for ABI (13% in the younger vs. 19% in the older group), LI (31 vs. 34%), and BH (26 vs. 15%).

Patient Outcome at Discharge

During the hospital stay (mean 61 days), 99 patients (5.7%) died: 73 died directly from stroke (36 BH, 24 CEI, 6 ABI, 7 OTI). Sixty-two percent of patients were graded in a good outcome category at discharge. A total of 241 patients received warfarin at discharge, and 499 received antiplatelet agents.

Prognosis within 3 Years after the Index Stroke

Of the 1,565 patients with follow-up data (a follow-up rate of 90%), 198 patients had a recurrent stroke, and 286 patients died within 3 years after the index stroke. Carotid endarterectomy and extracranial-intracranial bypass surgery were performed on 9 and 11 patients, respectively.

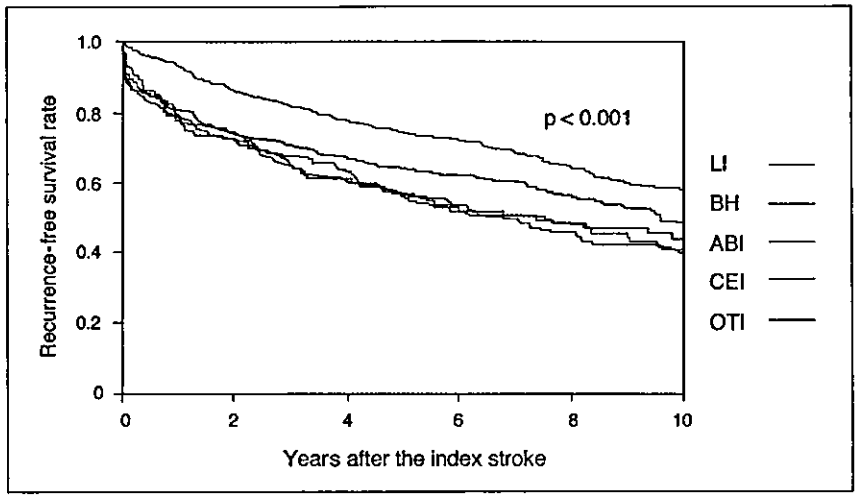

Fig. 1. Recurrence-free survival rate after the index stroke by subtypes. Kaplan-Meier analysis showed that significant differences were demonstrated in recurrence-free survival rates among stroke subtypes through the follow-up period as well as within 3 years after the stroke onset.

Table 2. Change in stroke subtype between the first and recurrent strokes within 3 years after the index stroke

Subtype of index stroke	Cases (n = 1,732)	Recurrence	Same subtype	Other subtype	
				ischemic	hemorrhagic
Ischemic stroke	1,382	172	105 (61)	56 (33)	11 (6)
ABI	287	37	24 (65)	11 (30)	2 (5)
LI	556	66	33 (50)	29 (44)	4 (6)
CEI	371	47	38 (81)	5 (11)	4 (8)
OTI	168	22	10 (45)	11 (50)	1 (5)
Hemorrhagic stroke, BH	350	26	12 (46)	14 (54)	–

$p < 0.05$. Figures in parentheses indicate percentages.

Significant differences in the recurrence-free survival rates were demonstrated among stroke subtypes (fig. 1). One hundred and one patients (6.5%) had the recurrent stroke within 1 year after the index stroke. The recurrence rate within the first year was significantly higher in CEI (9.0%) and OTI (9.1%) than in the other subtypes: 7.6% for ABI, 5.2% for LI, and 3.7% for BH. After the first year, the recurrence rate was not significantly different among the subtypes. A majority of the patients with stroke recurrences, particularly those with CEI, had a recurrent stroke of the same subtype as the index stroke (table 2). In time analyses, the recurrence-free survival within the initial year was not different during the initial and recent decades (84 vs. 86%). The recurrence-free survival within the first year was significantly lower in the older group than in the younger group (81 vs. 89%, $p < 0.05$).

Among a total of 1,466 stroke survivors, 199 patients died within 3 years after the discharge: 23 patients died of stroke, 42 of heart disease, 17 of cancer, and the remaining patients of other causes. In those survivors, a history of TIA, AF, IHD, and disability at discharge were significant predictors for recurrence or death after multivariate risk-adjusted estimation (table 3).

Discussion

This is the first hospital-based study in Japan that investigated long-term prognosis by stroke subtypes and identified the determinants of stroke recurrence or death in patients with a first-ever stroke.